Targeting the ATP-dependent formation of herpesvirus ribonucleoprotein particle assembly as an antiviral approach

Sophie Schumann, Brian R. Jackson, Ian Yule, Steven K. Whitehead, Charlotte Revill, Richard Foster and Adrian Whitehouse

Supplementary Figures 1-14.

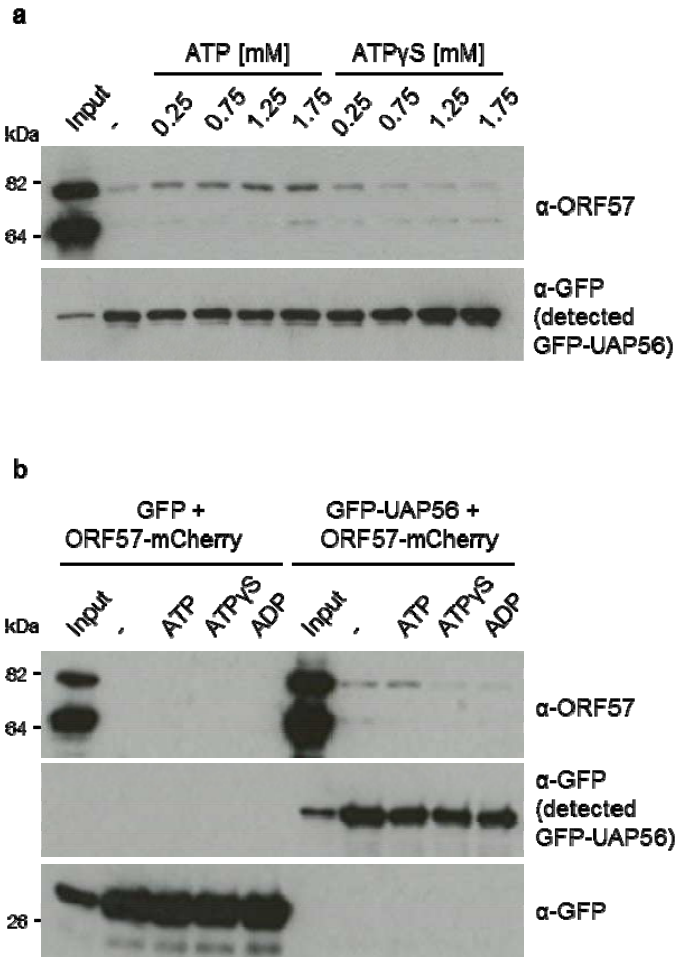

Supplementary Figure 1: Immunoprecipitations confirming the ATP-cycle dependent remodeling of hTREX and the effect of ORF57-mediated vRNP formation. (**a**) Immunoprecipitations of GFP-UAP56 after co-expression with mCherry-ORF57. Precipitations were performed with HEK-293T whole cell lysate (Input) in the absence of any additional nucleotides or with increasing concentrations of nucleotides, as indicated. Samples were analyzed by western blotting using the indicated antibodies. Results are representative of 3 independent repeats. (**b**) Immunoprecipitations of GFP or GFP-UAP56, co-expressed with mCherry-ORF57. Precipitations were performed with HEK-293T whole cell lysates (Input) in the absence of any additional nucleotides or in presence of 1.25 mM ATP, ATPγS, ADP. Samples were analyzed by western blotting using the indicated antibodies. Results are representative of 3 independent repeats.

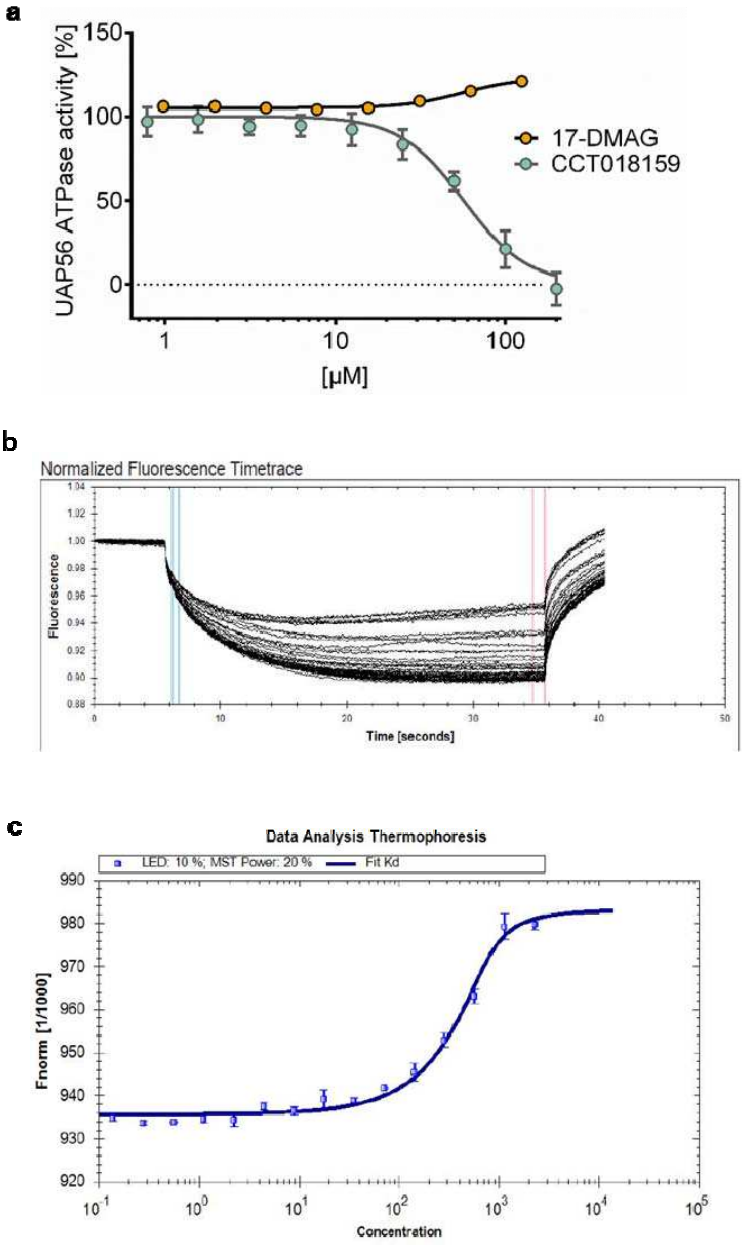

Supplementary Figure 2: UAP56 ATPase activity is not inhibited by 17-DMAG and microscale thermophoresis raw data showing binding of CCT018159 to UAP56. (**a**) Inhibition of UAP56 ATP-hydrolysis by 17-DMAG, compared to CCT018159. *In vitro* ATPase activity of purified recombinant UAP56 was measured in the presence of increasing concentrations of 17-DMAG. n = 3, error bars display the SD (SD is ≤ 2% for each value, therefore error bars not visible). Data for CCT018159 was taken from **Figure 2e**. (**b**) Normalized fluorescence timetrace (raw data) for UAP56 with varying concentrations of CCT018159. Indicated in blue and pink are the temperature jump regions, during which the IR laser generates a temperature gradient. The fluorescent timetrace indicates the thermophoretic trace of UAP56 before, during and after the temperature gradient. (**c**) Normalized fluorescence raw data for UAP56 during thermophoresis, shown as function of CCT018159 concentration. The curve and K_D were calculated by the NTanalysis software. n = 3, error bars display the SD.

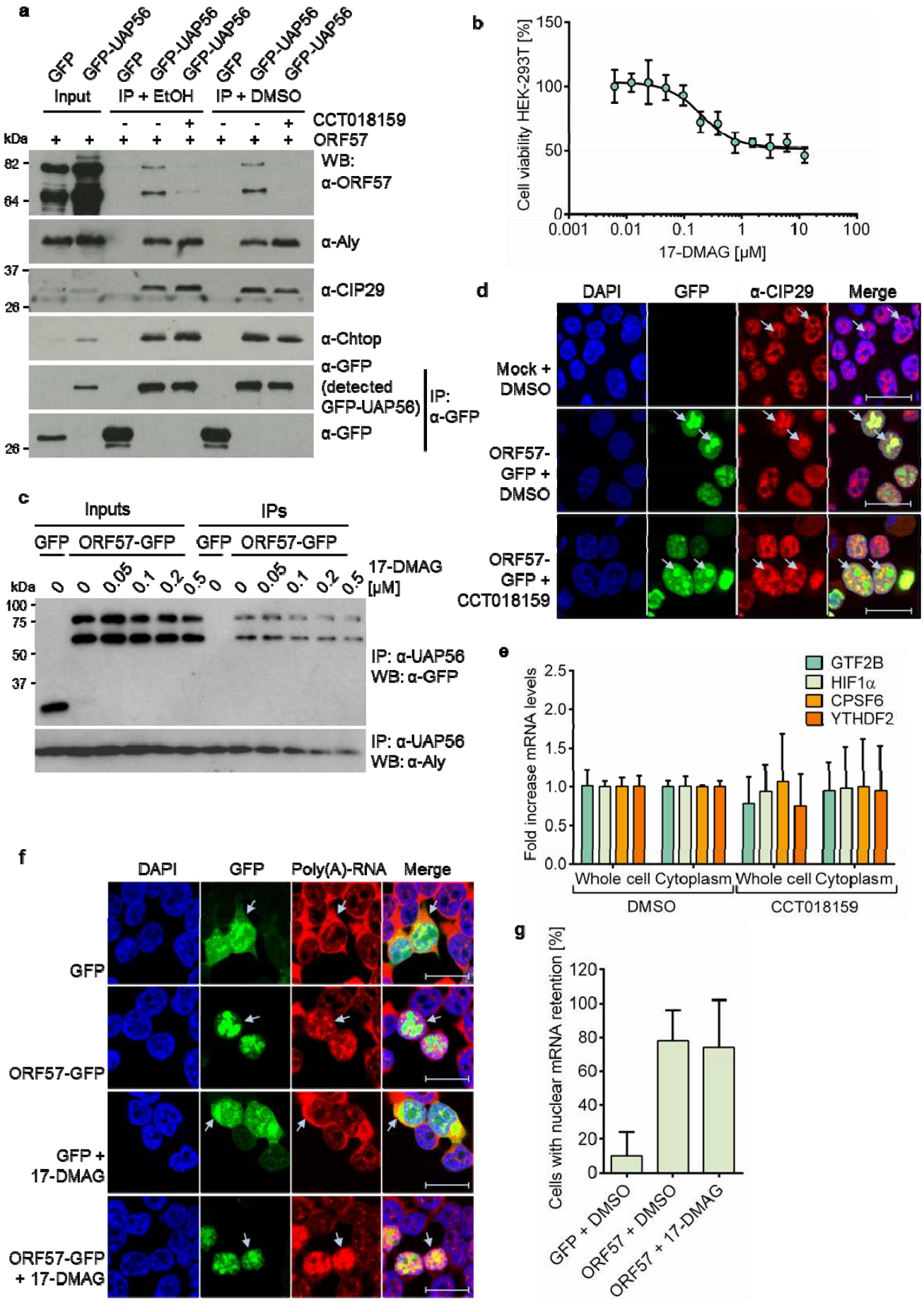
a
GFP
GFP-UAP56
Input
IP + EtOH
IP + DMSO
CCT018159
ORF57
kDa
82
64
37
26
WB: α-ORF57
α-Aly
α-CIP29
α-Chtop
α-GFP (detected GFP-UAP56)
IP: α-GFP
α-GFP
b
Cell viability HEK-293T [%]
17-DMAG [μM]
c
Inputs
IPs
17-DMAG [μM]
IP: α-UAP56 WB: α-GFP
IP: α-UAP56 WB: α-Aly
d
DAPI
GFP
α-CIP29
Merge
Mock + DMSO
ORF57-GFP + DMSO
ORF57-GFP + CCT018159
e
GTF2B
HIF1α
CPSF6
YTHDF2
Fold increase mRNA levels
Whole cell
Cytoplasm
DMSO
CCT018159
f
DAPI
GFP
Poly(A)-RNA
Merge
GFP
ORF57-GFP
GFP + 17-DMAG
ORF57-GFP + 17-DMAG
g
Cells with nuclear mRNA retention [%]
GFP + DMSO
ORF57 + DMSO
ORF57 + 17-DMAG

Supplementary Figure 3: Disruption of vRNP formation by CCT018159, but not by HSP90 inhibitor 17-DMAG. (**a**) Immunoprecipitations of GFP or GFP-UAP56 after co-expression with mCherry-ORF57. Precipitations were performed with HEK-293T whole cell lysates (Input) in the absence or in presence of 0.5 mM CCT018159 or Ethanol and DMSO as background control. Samples were analyzed by western blotting using the indicated antibodies. Results are representative of 2 independent repeats. (**b**) Cell viability of HEK-293T cells in the presence of increasing amounts of 17-DMAG as measured by MTS assay. Data was normalized to DMSO treated control cells. Values are averages, n = 5, error bars present SD. The CC_{50} was determined using non-linear regression with a variable slope (four-parameter logistic curve). (**c**) Immunoprecipitations of endogenous UAP56 after expression of GFP and ORF57-GFP. HEK-293T cells were treated with DMSO, or a concentration range of 17-DMAG as indicated, 6 h after transfection. Precipitations were performed with whole cell lysates (Input) in the absence or in presence of 17-DMAG. Samples were analyzed by western blotting using the indicated antibodies. Results are representative of 3 independent repeats with varying concentrations. (**d**) Confocal microscopy of HEK-293T cells either untransfected or expressing ORF57-GFP in the absence or presence of DMSO or 2.5 µM CCT018159, as indicated. Cells were stained using a CIP29-specific antibody and the nucleus visualized with DAPI. Arrows indicate the nucleolus. Scale bar = 20 µm. Images are representative of 2 independent repeats in HEK-293T cells and further 2 repeats in TREx BCBL1-Rta cells. (**e**) HEK-293T cells were treated with DMSO or 2.5 µM CCT018159 for 24 h. qRT-PCR was performed after subcellular fractionation. Transcript levels of GTF2B, HIF1α, CPSF6 and YTHDF2 were normalized to GAPDH and the relative increase calculated using the ΔΔCT method. Values are averages, n = 3, error bars display SD. (**f**) Cells expressing GFP or GFP-ORF57 were treated with DMSO or 0.1 µM 17-DMAG, as indicated. A fluorescently labelled oligo(dT) probe was used to detect poly(A) RNA, DAPI visualizes the nucleus. Arrows indicate localization of poly(A) RNA. Scale bar = 20 µm. Images representative of 2 independent experiments or more. (**g**) Quantification of cells with nuclear mRNA retention in GFP or ORF57-GFP transfected cells, treated with DMSO or 17-DMAG, as indicated. Values are averages of 4 independent experiments (GFP + DMSO), 6 independent experiments (ORF57-GFP + DMSO) or 2 independent experiments (ORF57-GFP + 17-DMAG), error bars present the SD. A total of 32 GFP transfected, 76 ORF57-GFP transfected cells treated with DMSO and 68 ORF57-GFP transfected cells treated with 17-DMAG were counted.

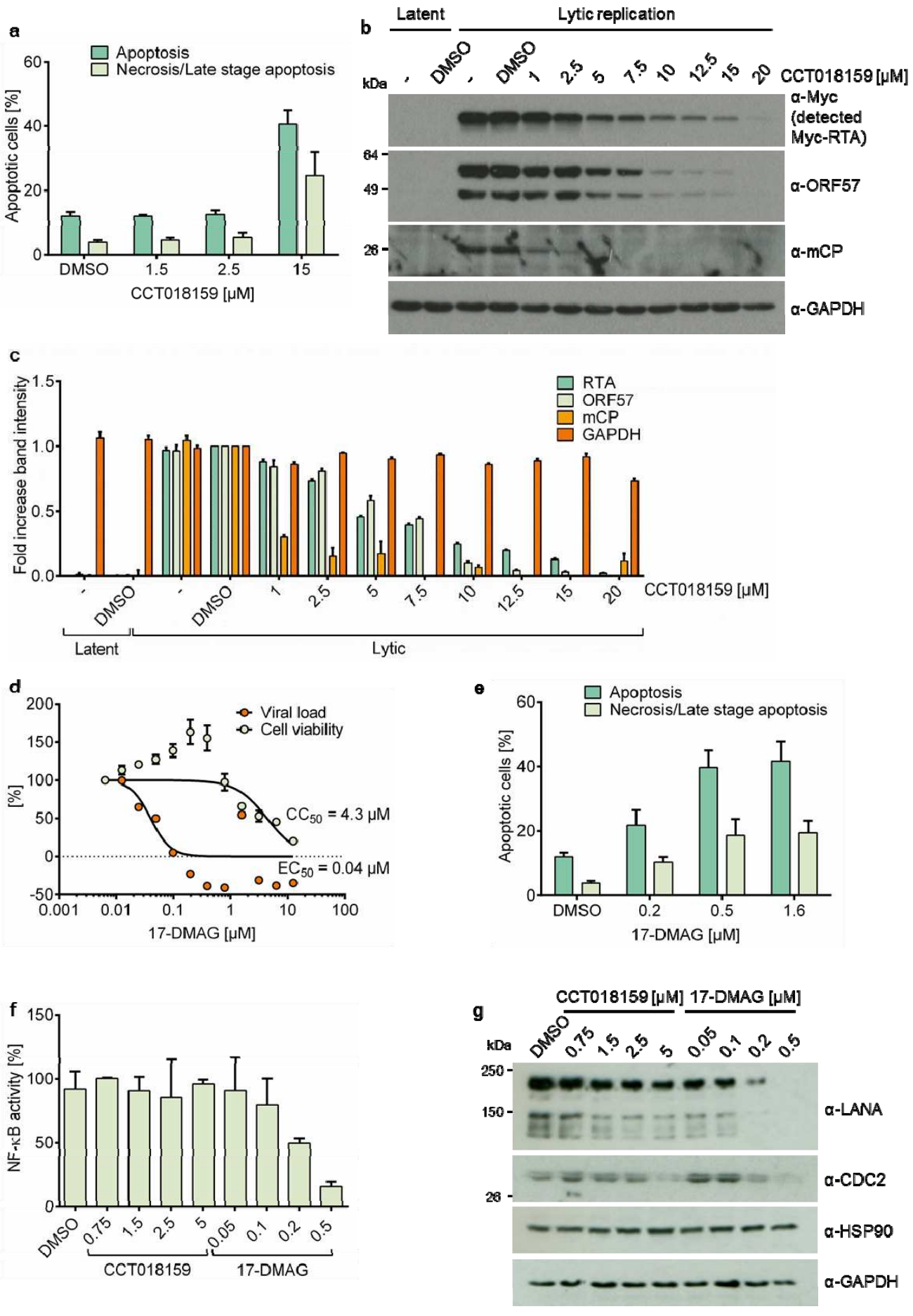
a
Apoptosis
Necrosis/Late stage apoptosis
Apoptotic cells [%]
60
40
20
0
DMSO
1.5
2.5
15
CCT018159 [μM]
b
Latent
Lytic replication
kDa
-
DMSO
-
DMSO
1
2.5
5
7.5
10
12.5
15
20
CCT018159 [μM]
α-Myc (detected Myc-RTA)
84
49
α-ORF57
28
α-mCP
α-GAPDH
c
Fold increase band intensity
1.5
1.0
0.5
0.0
RTA
ORF57
mCP
GAPDH
-
DMSO
-
DMSO
1
2.5
5
7.5
10
12.5
15
20
CCT018159 [μM]
Latent
Lytic
d
Viral load
Cell viability
[%]
200
150
100
50
0
-50
CC50 = 4.3 μM
EC50 = 0.04 μM
0.001
0.01
0.1
1
10
100
17-DMAG [μM]
e
Apoptosis
Necrosis/Late stage apoptosis
Apoptotic cells [%]
60
40
20
0
DMSO
0.2
0.5
1.6
17-DMAG [μM]
f
NF-κB activity [%]
150
100
50
0
DMSO
0.75
1.5
2.5
5
0.05
0.1
0.2
0.5
CCT018159
17-DMAG
g
CCT018159 [μM]
17-DMAG [μM]
kDa
DMSO
0.75
1.5
2.5
5
0.05
0.1
0.2
0.5
250
150
α-LANA
28
α-CDC2
α-HSP90
α-GAPDH

Supplementary Figure 4: Treatment with CCT018159 disrupts KSHV late protein expression, but shows a different phenotype for HSP90 inhibitor 17-DMAG. (**a**) Quantification of apoptosis in TREx BCBL1-Rta cells 72 h after treatment with DMSO or the indicated amounts of CCT018159. Cells were stained using Annexin V and propidium iodide to detect apoptotic and necrotic/late apoptotic cells before being counted by flow cytometry, assessing ≥ 50,000 cells. Values are averages, error bars present SD, n = 4 (DMSO treated) or n = 5 (CCT018159 treated). (**b**) Expression of KSHV immediate early and late proteins, as well as GAPDH in TREx BCBL1-Rta cells, 24 h after treatment with indicated amounts of CCT018159. Western blotting was analyzed using Myc-specific antibodies to detect Myc-Rta and ORF57-, mCP- and GAPDH-specific antibodies to detect the indicated proteins. Results are representative of 3 repeats (at varying concentrations). (**c**) Quantification of western blot band intensities used to generate the CC_{50} in **Figure 4c**. Values are averages, error bars present SD, n = 3. (**d**) Cell viability and viral load in TREx BCBL1-Rta cells in response to 17-DMAG. Viability 72 h after treatment with 17-DMAG was determined by MTS assay. Values are averages, error bars present SD, n = 5. The viral load was measured by qPCR, 72 h after induction of KSHV lytic replication and treatment with 17-DMAG. Viral DNA was normalized to GAPDH and the relative decrease compared to DMSO treated samples calculated using the ΔΔCT method. EC_{50} and CC_{50} values were determined using non-linear regression with a variable slope (normalized response). (**e**) Quantification of apoptosis in TREx BCBL1-Rta cells 72 h after treatment with DMSO or the indicated amounts of 17-DMAG. Cells were stained using Annexin V and propidium iodide to detect apoptotic and necrotic cells before being counted by flow cytometry, assessing ≥ 50,000 cells. Values are averages, error bars present SD, n = 4 (DMSO treated) or n = 3 (17-DMAG treated). (**f**) NF-κB signaling activity 24 h after treatment with DMSO or a concentration range of CCT018159 or 17-DMAG, as indicated. NF-κB activity was determined after nucleofection of a reporter plasmid expressing firefly luciferase under the control of the NF-κB elements from the concanavalin A promotor. Values were normalized to Renilla luciferase, expressed from the pRLTK reporter plasmid, which was used as control for transfection efficiency. Values are averages, error bars present SD of 3 independent experiments, each with n = 3. (**g**) Expression of KSHV LANA and the cellular proteins CDC2, HSP90 and GAPDH by TREx BCBL1-Rta cells 72 h after treatment with DMSO or a concentration range of CCT018159 or 17-DMAG, as indicated. Samples were analyzed by western blotting using the indicated antibodies. Results are representative of 2 independent repeats.

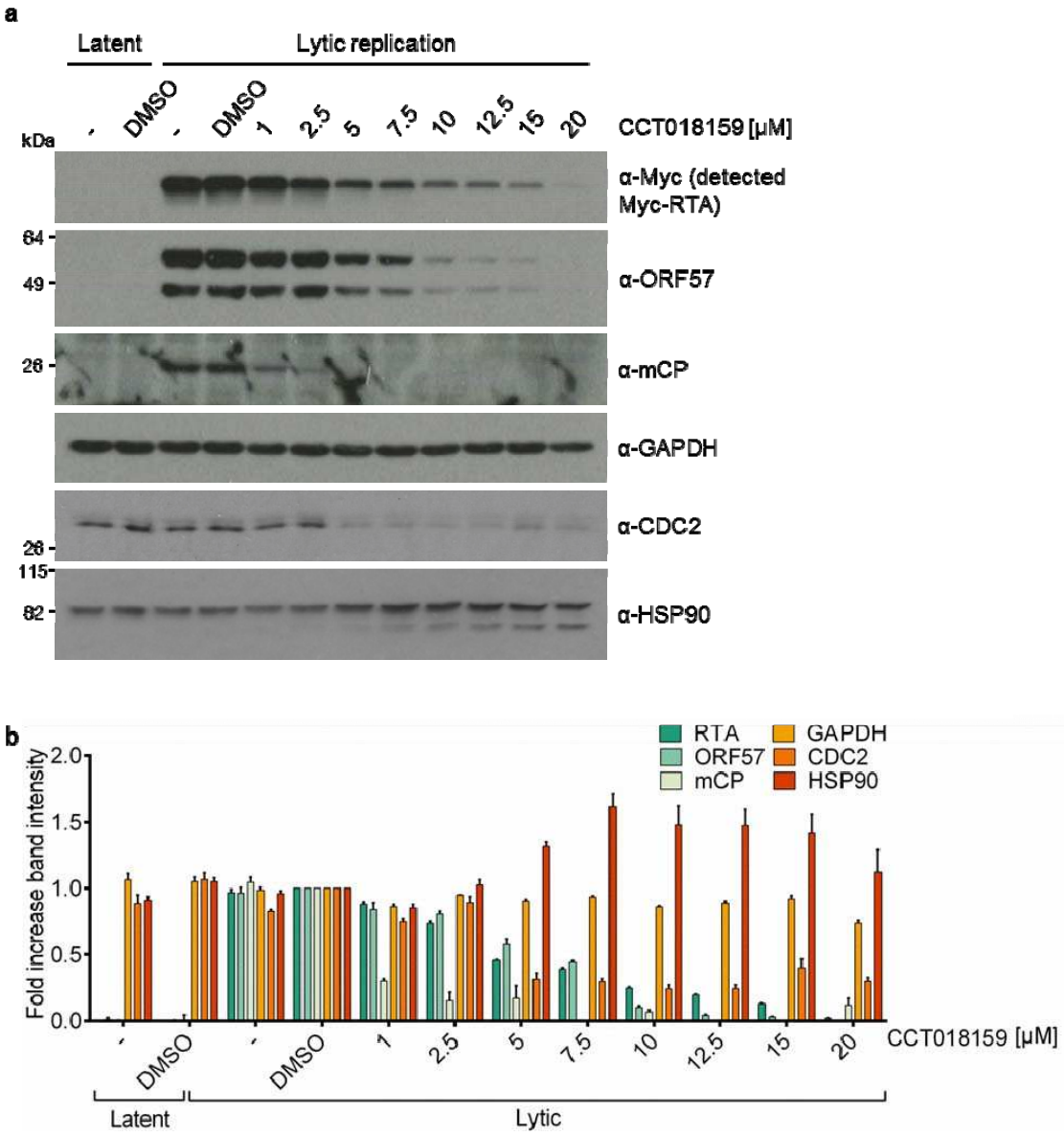

Supplementary Figure 5: Effect of CCT018159 on HSP90 in TREx BCBL1-Rta cells. (**a**) Western blots of TREx BCBL1-Rta cell lysates shown in **Supplementary Figure 4b** were also probed for expression of HSP90 and HSP90 client protein CDC2 using protein-specific antibodies. Results are representative of ≥ 2 independent repeats. (**b**) Quantification of western blot band intensities. Values are averages, error bars present SD, n = 3. (**c**) Expression of KSHV late protein mCP compared to expression of CDC2 in TREx BCBL1-Rta cells, after treatment with indicated concentrations of CCT018159. Values are averages, error bars present SD, n = 3. Curves were determined using non-linear regression with a variable slope (four-parameter logistic curve).

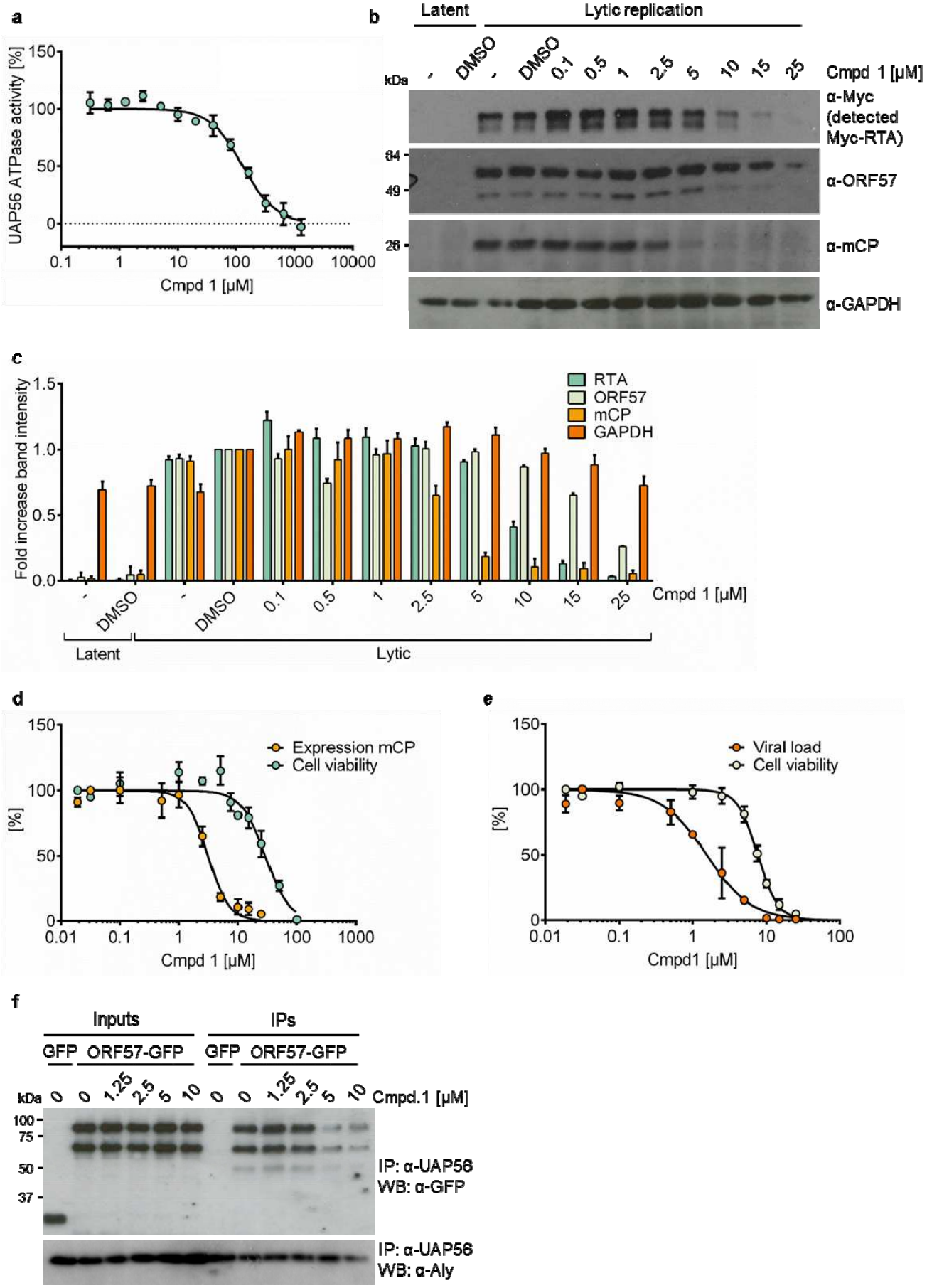
a
UAP56 ATPase activity [%]
150
100
50
0
0.1
1
10
100
1000
10000
Cmpd 1 [µM]
b
Latent
Lytic replication
kDa
-
DMSO
-
DMSO
0.1
0.5
1
2.5
5
10
15
25
Cmpd 1 [µM]
α-Myc (detected Myc-RTA)
64
49
α-ORF57
28
α-mCP
α-GAPDH
c
Fold increase band intensity
1.5
1.0
0.5
0.0
RTA
ORF57
mCP
GAPDH
-
DMSO
-
DMSO
0.1
0.5
1
2.5
5
10
15
25
Cmpd 1 [µM]
Latent
Lytic
d
150
100
50
0
[%]
Expression mCP
Cell viability
0.01
0.1
1
10
100
1000
Cmpd 1 [µM]
e
150
100
50
0
[%]
Viral load
Cell viability
0.01
0.1
1
10
100
Cmpd1 [µM]
f
Inputs
IPs
GFP
ORF57-GFP
GFP
ORF57-GFP
kDa
0
0
1.25
2.5
5
10
0
0
1.25
2.5
5
10
Cmpd.1 [µM]
100
75
50
37
IP: α-UAP56
WB: α-GFP
IP: α-UAP56
WB: α-Aly

Supplementary Figure 6: Effect of Compound 1 on KSHV lytic replication and cell viability. (**a**) *In vitro* ATPase activity of purified UAP56, in the presence of increasing concentrations of Compound 1. Values are averages, error bars display the SD, n = 3. The IC_{50} was determined using non-linear regression with a variable slope (four-parameter logistic curve). (**b**) Expression of KSHV immediate early and late proteins, as well as GAPDH in TREx BCBL1-Rta cells, 24 h after treatment with indicated amounts of Compound 1. Western blotting was analyzed using Myc-specific antibodies to detect Myc-Rta and ORF57-, mCP- and GAPDH-specific antibodies to detect the indicated proteins. Results are representative of 2 independent repeats. (**c**) Quantification of western blot band intensities used to generate the EC_{50}. Values are averages, error bars present SD, n = 3. (**d**) Expression of viral late protein mCP after normalization to GAPDH and cell viability in TREx BCBL1-Rta cells, after treatment with indicated concentrations of Compound 1. Values are averages, error bars present SD, n ≥ 3. CC_{50} and EC_{50} values were determined using non-linear regression with a variable slope (four-parameter logistic curve). (**e**) Viral load and cell viability in TREx BCBL1-Rta cells in the presence of Compound 1, 72 h after induction of KSHV lytic replication. Viral DNA was quantified by qPCR, normalized to GAPDH and the relative decrease compared to DMSO treated samples calculated using the ΔΔCT method. Values are averages, error bars present SD, n ≥ 3. CC_{50} and EC_{50} values were determined using non-linear regression with a variable slope (four-parameter logistic curve). (**f**) Immunoprecipitations of endogenous UAP56 in GFP or ORF57-GFP expressing cells. HEK-293T cells were treated with indicated amounts of Compound 1, 6 h after transfection. Precipitations were performed with whole cell lysates (Input) in the absence or in presence of the indicated Compound 1 concentration range or DMSO control. Samples were analyzed by western blotting using the indicated antibodies. Results are representative of 2 independent repeats.

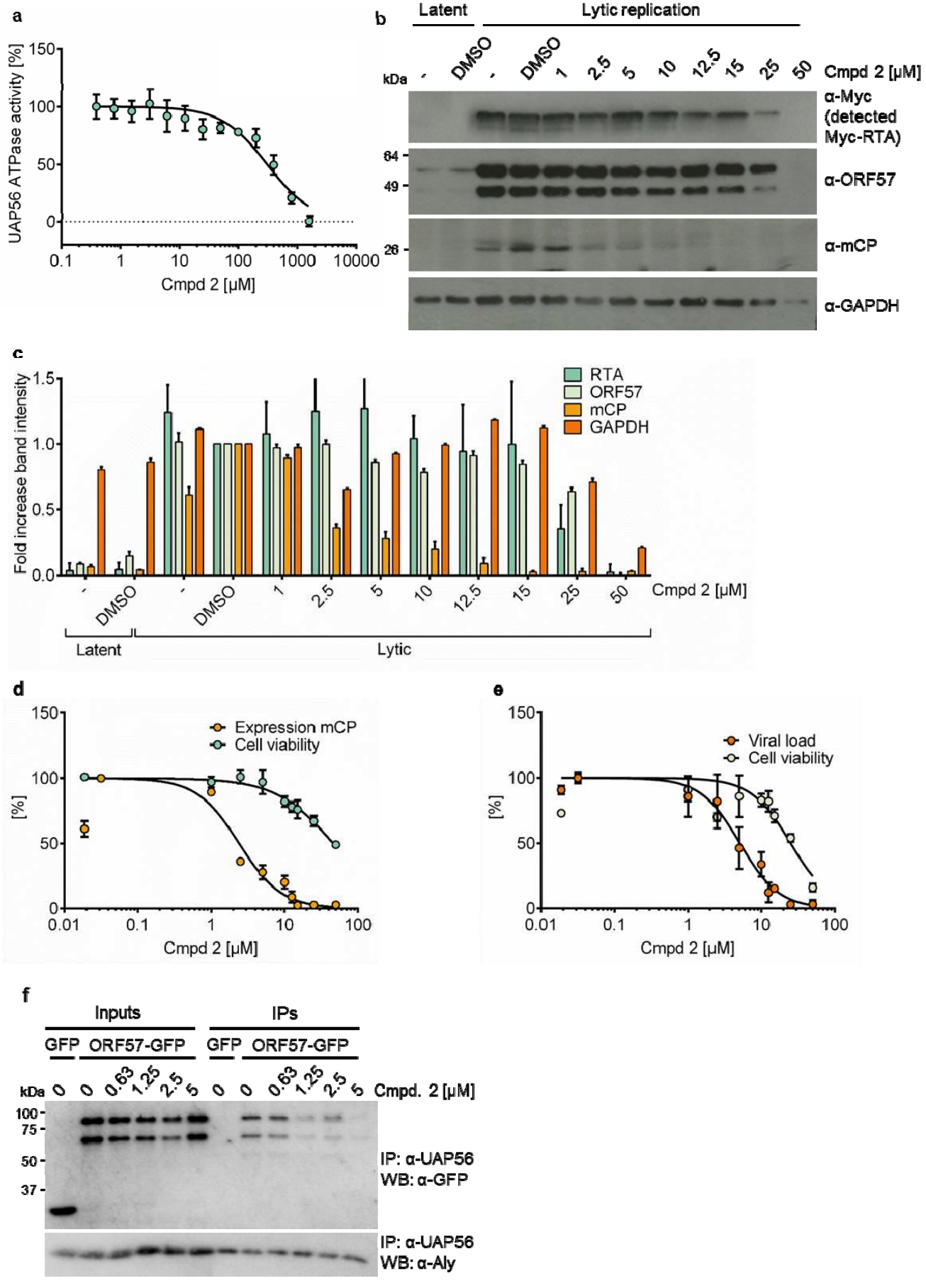
a
UAP56 ATPase activity [%]
150
100
50
0
0.1
1
10
100
1000
10000
Cmpd 2 [µM]
b
Latent
Lytic replication
kDa
-
DMSO
-
DMSO
1
2.5
5
10
12.5
15
25
50
Cmpd 2 [µM]
α-Myc (detected Myc-RTA)
64
49
α-ORF57
28
α-mCP
α-GAPDH
c
Fold increase band intensity
1.5
1.0
0.5
0.0
RTA
ORF57
mCP
GAPDH
-
DMSO
-
DMSO
1
2.5
5
10
12.5
15
25
50
Cmpd 2 [µM]
Latent
Lytic
d
Expression mCP
Cell viability
[%]
150
100
50
0
0.01
0.1
1
10
100
Cmpd 2 [µM]
e
Viral load
Cell viability
[%]
150
100
50
0
0.01
0.1
1
10
100
Cmpd 2 [µM]
f
Inputs
IPs
GFP
ORF57-GFP
GFP
ORF57-GFP
kDa
0
0
0.63
1.25
2.5
5
0
0
0.63
1.25
2.5
5
Cmpd. 2 [µM]
100
75
50
37
IP: α-UAP56
WB: α-GFP
IP: α-UAP56
WB: α-Aly

Supplementary Figure 7: Effect of Compound 2 on KSHV lytic replication and cell viability. (**a**) *In vitro* ATPase activity of purified UAP56, in the presence of increasing concentrations of Compound 2. Values are averages from two assays performed after two independent protein purifications. n = 6, error bars display the SD. The IC_{50} was determined using non-linear regression with a variable slope (four-parameter logistic curve). (**b**) Expression of KSHV immediate early and late proteins, as well as GAPDH in TREx BCBL1-Rta cells, 24 h after treatment with Compound 2. Western blotting was analyzed using Myc-specific antibodies to detect Myc-Rta and ORF57-, mCP- and GAPDH-specific antibodies to detect the indicated proteins. Results are representative of 2 independent repeats. (**c**) Quantification of western blot band intensities used to generate the EC_{50}. Values are averages, error bars present SD, n = 3. (**d**) Expression of viral late protein mCP after normalization to GAPDH and cell viability in TREx BCBL1-Rta cells, after treatment with Compound 2. Values are averages, error bars present SD, n ≥ 3. CC_{50} and EC_{50} values were determined using non-linear regression with a variable slope (four-parameter logistic curve). (**e**) Viral load and cell viability in TREx BCBL1-Rta cells in the presence of Compound 2, 72 h after induction of KSHV lytic replication. Viral DNA was quantified by qPCR, normalized to GAPDH and the relative decrease compared to DMSO treated samples calculated using the ΔΔCT method. Values are averages, error bars present SD, n ≥ 4. CC_{50} and EC_{50} values were determined using non-linear regression with a variable slope (four-parameter logistic curve). (**f**) Immunoprecipitations of endogenous UAP56 in GFP or ORF57-GFP expressing cells. HEK-293T cells were treated with indicated amounts of Compound 2, 6 h after transfection. Precipitations were performed with whole cell lysates (Input) in the absence or in presence of the indicated Compound 2 concentration range or DMSO control. Samples were analyzed by western blotting using the indicated antibodies. Results are representative of 2 independent repeats.

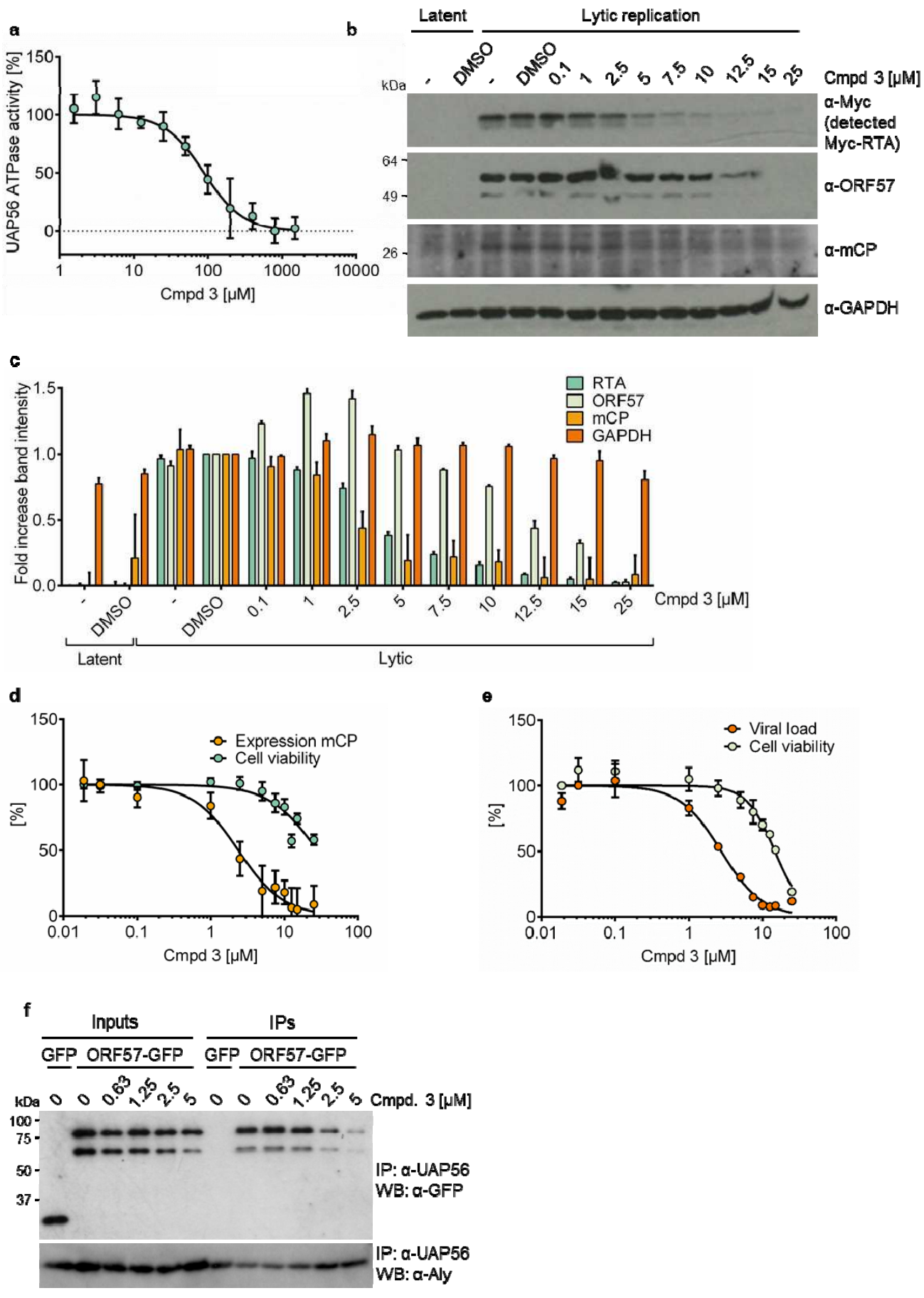
a
UAP56 ATPase activity [%]
150
100
50
0
1
10
100
1000
10000
Cmpd 3 [µM]
b
Latent
Lytic replication
kDa
-
DMSO
-
DMSO
0.1
1
2.5
5
7.5
10
12.5
15
25
Cmpd 3 [µM]
64
49
26
α-Myc (detected Myc-RTA)
α-ORF57
α-mCP
α-GAPDH
c
Fold increase band intensity
1.5
1.0
0.5
0.0
RTA
ORF57
mCP
GAPDH
-
DMSO
-
DMSO
0.1
1
2.5
5
7.5
10
12.5
15
25
Cmpd 3 [µM]
Latent
Lytic
d
[%]
150
100
50
0
Expression mCP
Cell viability
0.01
0.1
1
10
100
Cmpd 3 [µM]
e
[%]
150
100
50
0
Viral load
Cell viability
0.01
0.1
1
10
100
Cmpd 3 [µM]
f
Inputs
IPs
GFP
ORF57-GFP
GFP
ORF57-GFP
kDa
0
0
0.63
1.25
2.5
5
0
0
0.63
1.25
2.5
5
Cmpd. 3 [µM]
100
75
50
37
IP: α-UAP56
WB: α-GFP
IP: α-UAP56
WB: α-Aly

Supplementary Figure 8: Effect of Compound 3 on KSHV lytic replication and cell viability. (**a**) *In vitro* ATPase activity of purified UAP56, in the presence of increasing concentrations of Compound 3. Values are averages from two assays performed after two independent protein purifications. n = 4, error bars display the SD. The IC_{50} was determined using non-linear regression with a variable slope (four-parameter logistic curve). (**b**) Expression of KSHV immediate early and late proteins, as well as GAPDH in TREx BCBL1-Rta cells, 24 h after treatment with Compound 3. Western blotting was analyzed using Myc-specific antibodies to detect Myc-Rta and ORF57-, mCP- and GAPDH-specific antibodies to detect the indicated proteins. Results are representative of 2 independent repeats (at varying concentrations). (**c**) Quantification of western blot band intensities used to generate the EC_{50}. Values are averages, error bars present SD, n = 3. (**d**) Expression of viral late protein mCP after normalization to GAPDH and cell viability in TREx BCBL1-Rta cells, after treatment with Compound 3. Values are averages, error bars present SD, n ≥ 3. CC_{50} and EC_{50} values were determined non-linear regression with a variable slope (four-parameter logistic curve). (**e**) Viral load and cell viability in TREx BCBL1-Rta cells in the presence of Compound 3, 72 h after induction of KSHV lytic replication. Viral DNA was quantified by qPCR, normalized to GAPDH and the relative decrease compared to DMSO treated samples calculated using the ΔΔCT method. Values are averages, error bars present SD, n ≥ 2. CC_{50} and EC_{50} values were determined using non-linear regression with a variable slope (four-parameter logistic curve). (**f**) Immunoprecipitations of endogenous UAP56 in GFP or ORF57-GFP expressing cells. HEK-293T cells were treated with indicated amounts of Compound 3, 6 h after transfection. Precipitations were performed with whole cell lysates (Input) in the absence or in presence of the indicated Compound 3 concentration range or DMSO control. Samples were analyzed by western blotting using the indicated antibodies. Results are representative of 2 independent repeats.

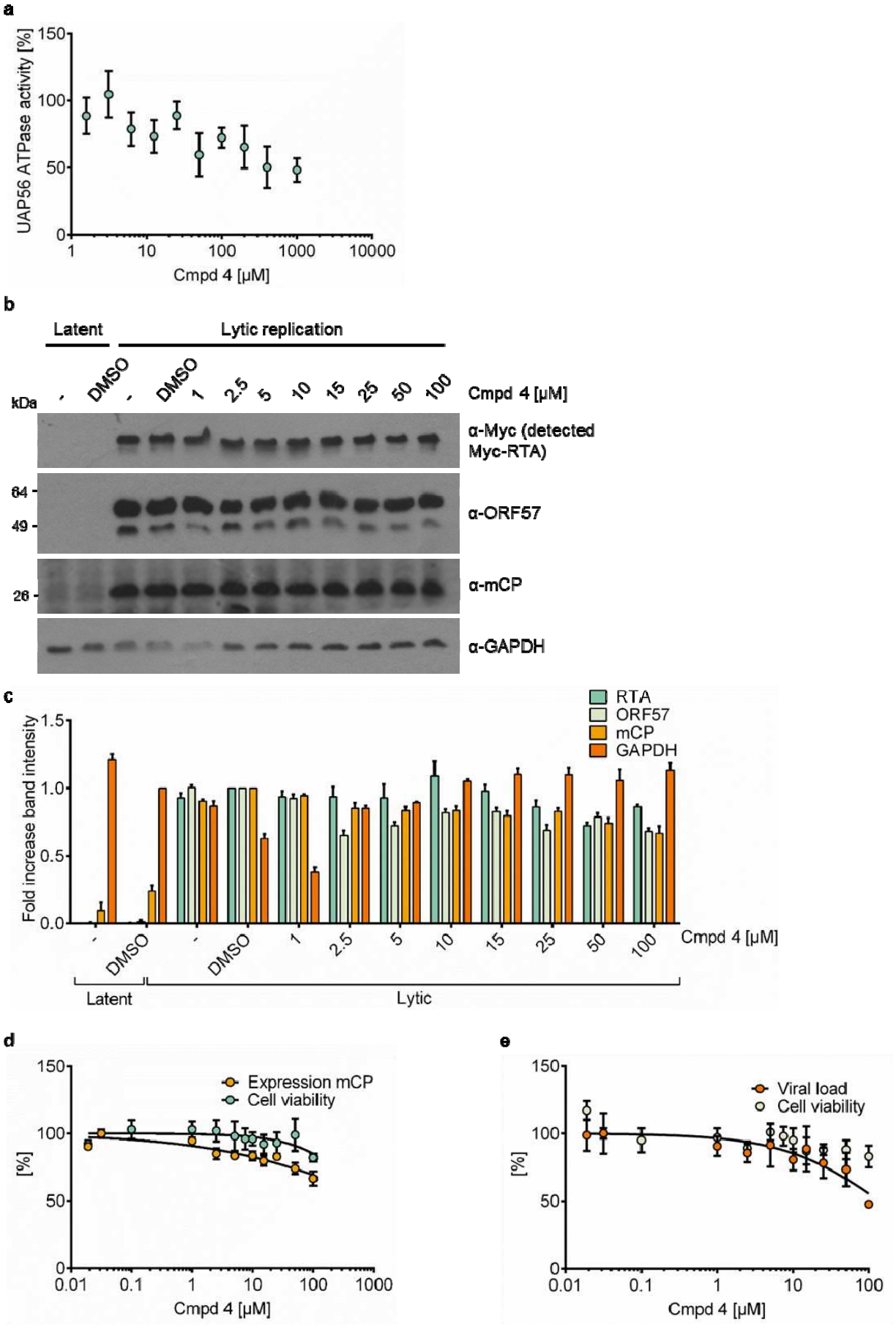
a
UAP56 ATPase activity [%]
150
100
50
0
1
10
100
1000
10000
Cmpd 4 [µM]
b
Latent
Lytic replication
kDa
-
DMSO
-
DMSO
1
2.5
5
10
15
25
50
100
Cmpd 4 [µM]
α-Myc (detected Myc-RTA)
64
49
α-ORF57
26
α-mCP
α-GAPDH
c
RTA
ORF57
mCP
GAPDH
Fold increase band intensity
1.5
1.0
0.5
0.0
-
DMSO
-
DMSO
1
2.5
5
10
15
25
50
100
Cmpd 4 [µM]
Latent
Lytic
d
Expression mCP
Cell viability
[%]
150
100
50
0
0.01
0.1
1
10
100
1000
Cmpd 4 [µM]
e
Viral load
Cell viability
[%]
150
100
50
0
0.01
0.1
1
10
100
Cmpd 4 [µM]

Supplementary Figure 9: Effect of Compound 4 on KSHV lytic replication and cell viability. (**a**) *In vitro* ATPase activity of purified UAP56, in the presence of increasing concentrations of Compound 4. Values are averages from two assays performed after two independent protein purifications. n = 6, error bars display the SD. No IC_{50} could be determined using non-linear regression. (**b**) Expression of KSHV immediate early and late proteins, as well as GAPDH in TREx BCBL1-Rta cells, 24 h after treatment with indicated amounts of Compound 4. Western blotting was analyzed using Myc-specific antibodies to detect Myc-Rta and ORF57-, mCP- and GAPDH-specific antibodies to detect the indicated proteins. Results are representative of 2 independent repeats (at varying concentrations). (**c**) Quantification of western blot band intensities used to generate the EC_{50}. Values are averages, error bars present SD, n = 3. (**d**) Expression of viral late protein mCP after normalization to GAPDH and cell viability in TREx BCBL1-Rta cells, after treatment with indicated concentrations of Compound 4. Values are averages, error bars present SD, n ≥ 3. CC_{50} and EC_{50} values were extrapolated using non-linear regression with a variable slope (four-parameter logistic curve). (**e**) Viral load and cell viability in TREx BCBL1-Rta cells in the presence of Compound 4, 72 h after induction of KSHV lytic replication. Viral DNA was quantified by qPCR, normalized to GAPDH and the relative decrease compared to DMSO treated samples calculated using the ΔΔCT method. Values are averages, error bars present SD, n ≥ 2. The EC_{50} value was determined using non-linear regression with a variable slope (four-parameter logistic curve). No CC_{50} could be determined using non-linear regression, as the data points were found not to converge.

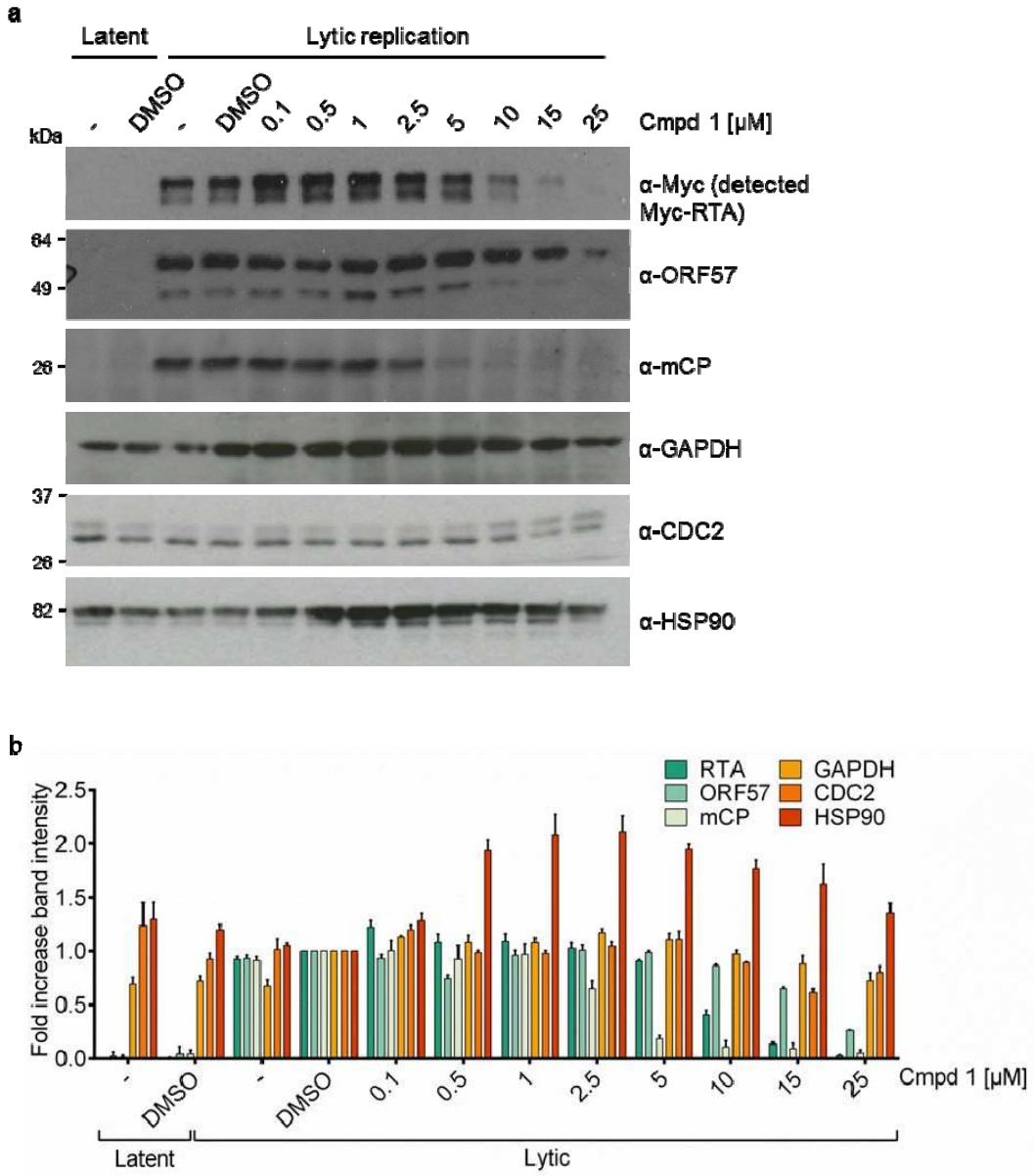

Supplementary Figure 10: Effect of Compound 1 on HSP90 in TREx BCBL1-Rta cells. (**a**) Western blots of TREx BCBL1-Rta cell lysates shown in **Supplementary Figure 6b** were also probed for expression of HSP90 and HSP90 client protein CDC2 using protein-specific antibodies. Results are representative of 2 independent repeats. (**b**) Quantification of western blot band intensities. Values are averages, error bars present SD, n = 3. (**c**) Expression of KSHV late protein mCP compared to expression of CDC2 in TREx BCBL1-Rta cells, after treatment with indicated concentrations of Compound 1. Values are averages, error bars present SD, n = 3. Curves were determined using non-linear regression with a variable slope (four-parameter logistic curve).

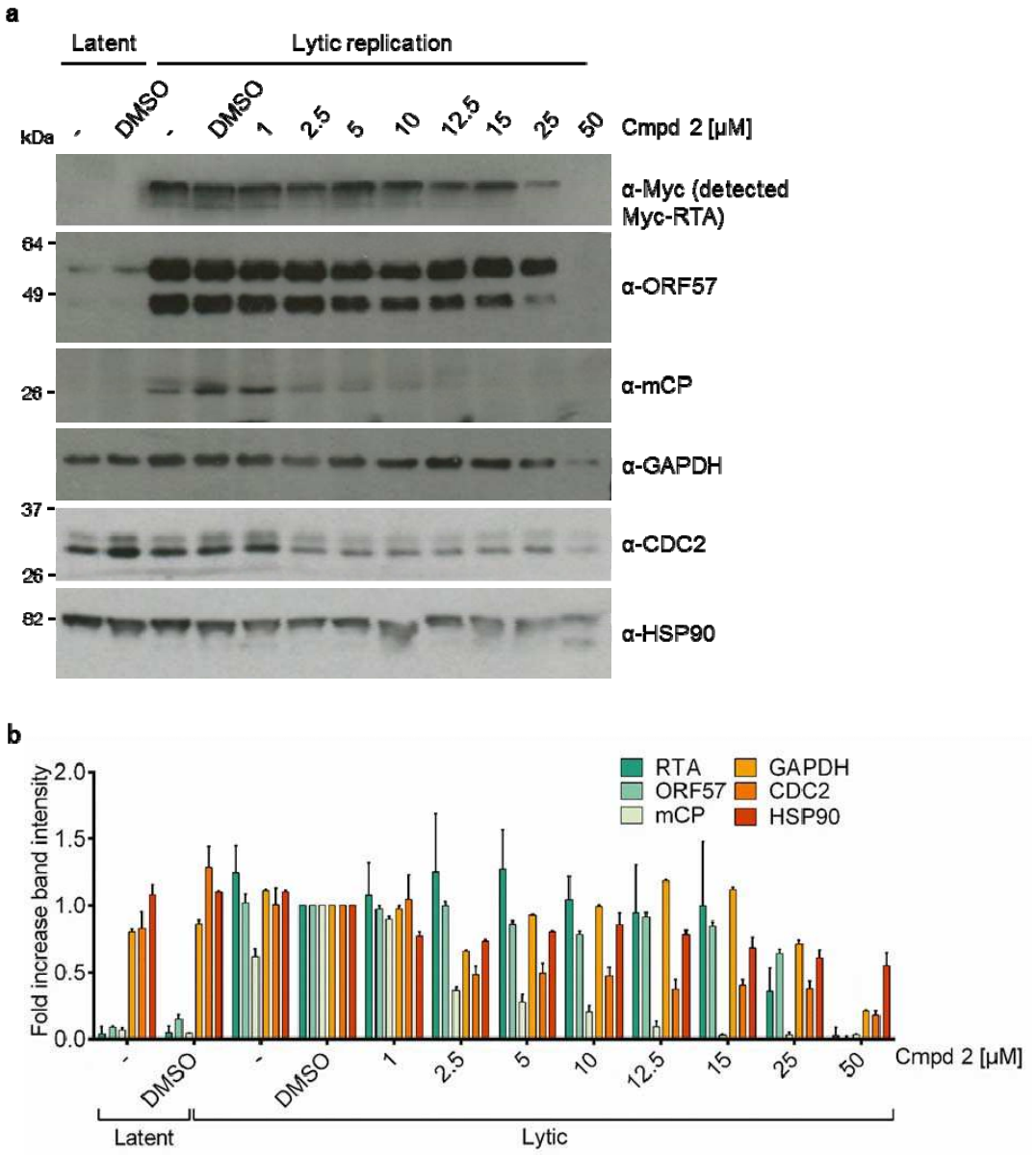

Supplementary Figure 11: Effect of Compound 2 on HSP90 in TREx BCBL1-Rta cells. (**a**) Western blots of TREx BCBL1-Rta cell lysates shown in **Supplementary Figure 7b** were also probed for expression of HSP90 and HSP90 client protein CDC2 using protein-specific antibodies. Results are representative of 2 independent repeats. (**b**) Quantification of western blot band intensities. Values are averages, error bars present SD, n = 3. (**c**) Expression of KSHV late protein mCP compared to expression of CDC2 in TREx BCBL1-Rta cells, after treatment with indicated concentrations of Compound 2. Values are averages, error bars present SD, n = 3. Curves were generated using non-linear regression with a variable slope (four-parameter logistic curve).

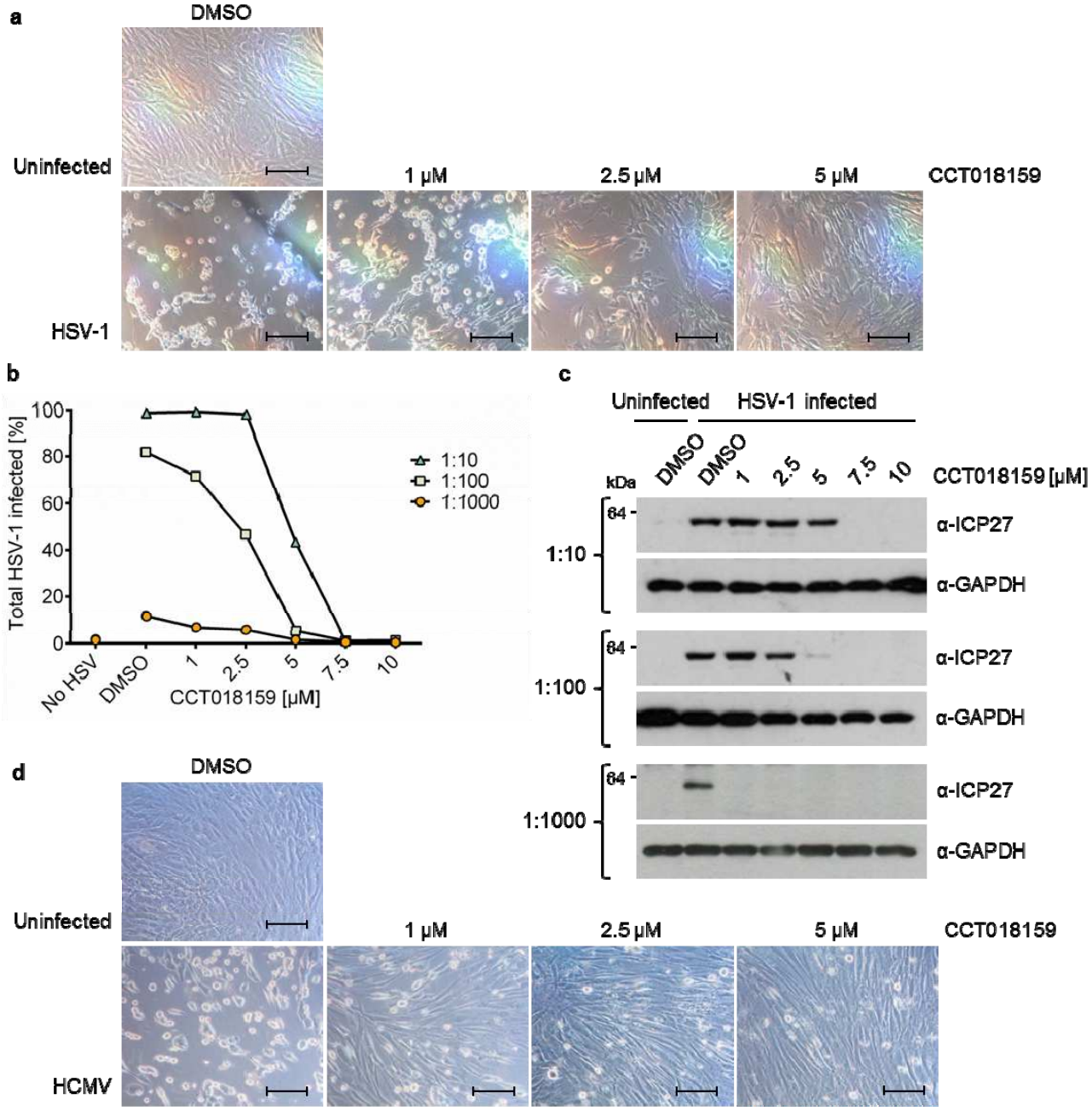

Supplementary Figure 12: CCT018159 disrupts HSV-1 and HCMV lytic replication in HFF cells. (**a**) Imaging of HFF cells after primary infection with HSV-1 for 72 h or uninfected cells treated with DMSO or the indicated amounts of CCT018159. Scale bar = 100 µm. Results are representative of 2 independent repeats. (**b**) Production of infectious HSV-1 virions was measured by re-infection of HFF cells, 72 h after primary infection and treatment with CCT018159. Supernatants of primary infected cells were diluted 1:10-1:1000 before being added to fresh HFF cells. The percentage of infected cells was determined by flow cytometry, assessing ≥ 10,000 cells. (**c**) HSV-1 infectious virion production and re-infection levels were confirmed by analysis of HSV-1 protein production. Virion containing supernatants were used to re-infect HFF cells at the indicated dilutions, 72 h after primary infection and treatment with CCT018159. Western blots were analyzed using ICP27- and GAPDH-specific antibodies to detect the indicated proteins. Results show dilutions of 3 biological repeats. (**d**) HFF cells after primary infection with HCMV for 120 h or uninfected cells treated with DMSO or the indicated amounts of CCT018159. Scale bar = 100 µm. Results are representative of 2 independent repeats.

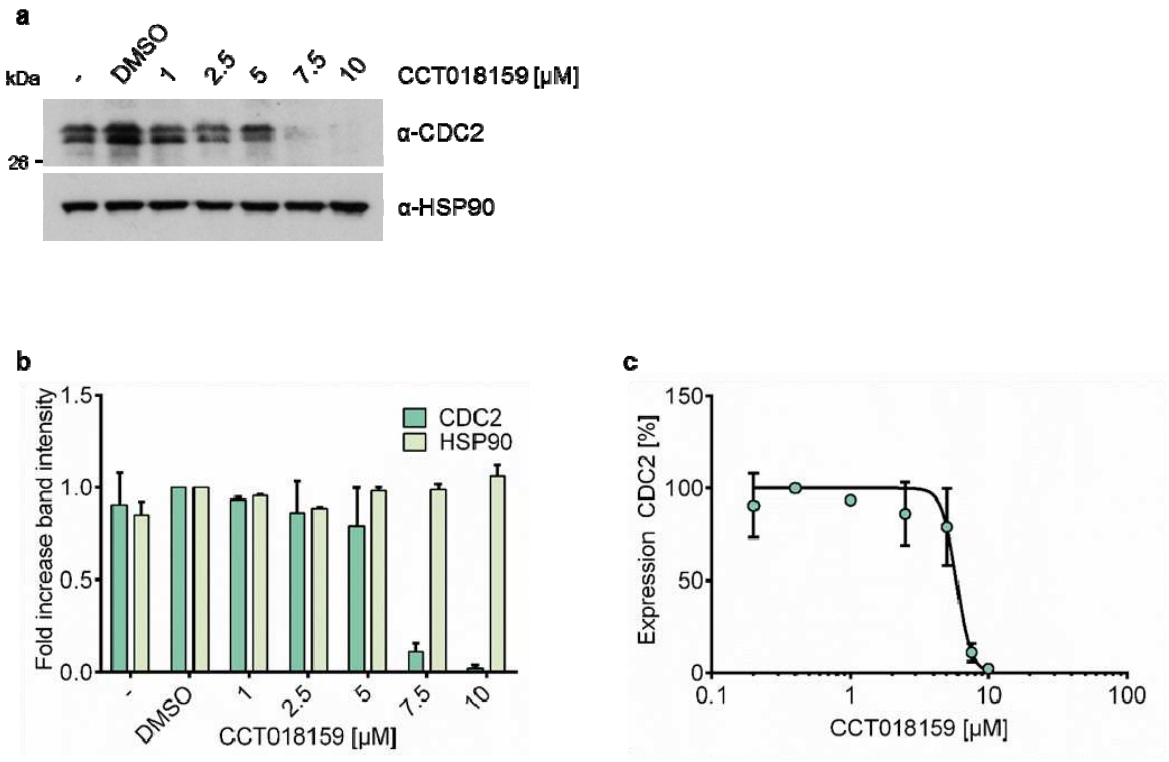

Supplementary Figure 13: Effect of CCT018159 on HSP90 in HFF cells. (**a**) Expression of HSP90 and HSP90 client protein CDC2 in HFF cells, 72 h after treatment with indicated amounts of CCT018159. Western blotting was analyzed using HSP90- and CDC2-specifc antibodies to detect indicated proteins. Results are representative of 2 repeats. (**b**) Quantification of western blot band intensities. Values are averages, error bars present SD, n = 3. (**c**) The CDC2 expression curve was generated using non-linear regression with a variable slope (four-parameter logistic curve).

Figure 1a

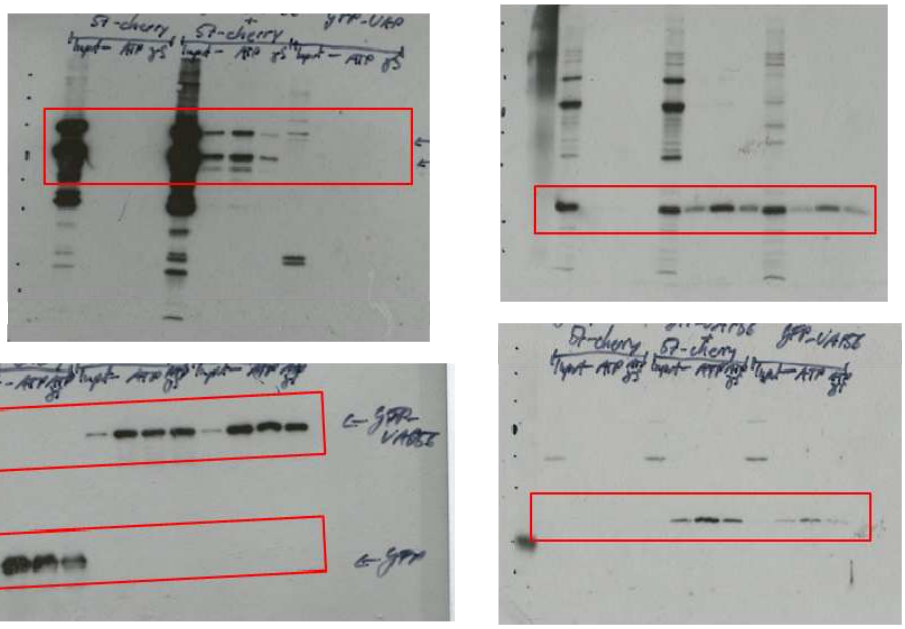

Figure 1c

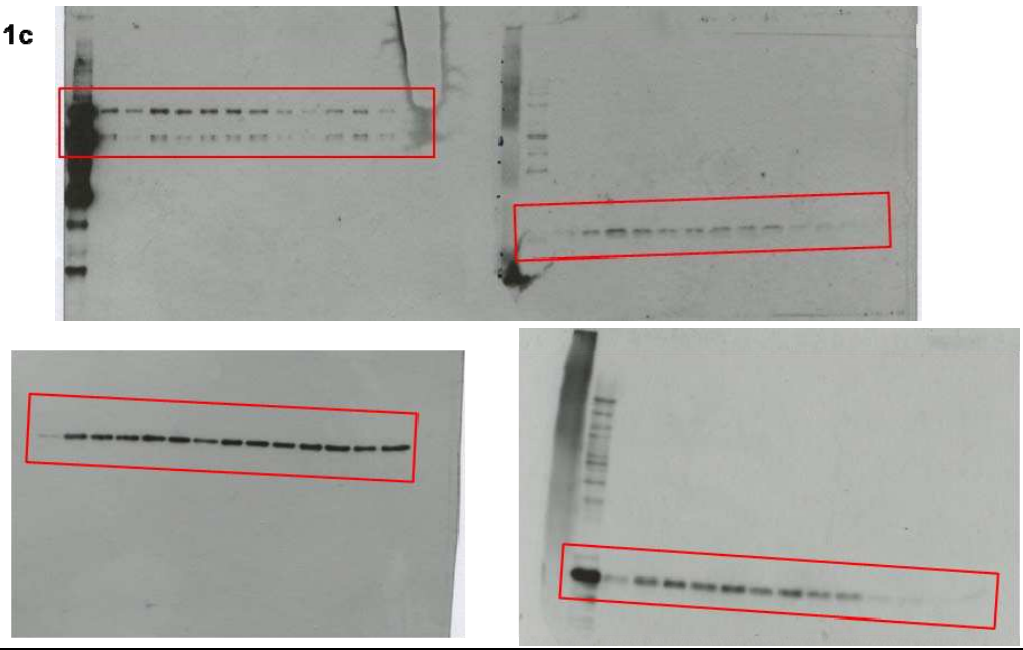

Figure 3 b

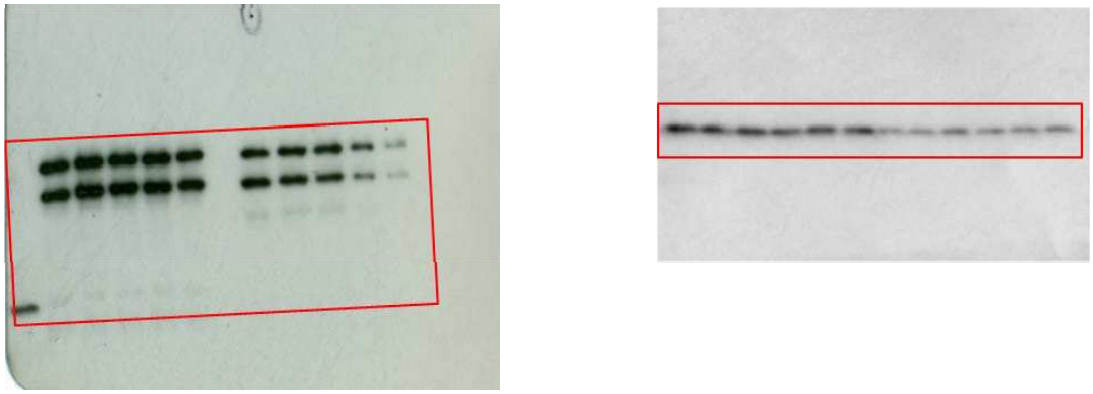

Supplementary Figure 14: Raw data presentation. Uncropped and unprocessed scans of all immunoblots. Labels indicate the corresponding figures, relevant bands are marked by the red box.

Figure 6a

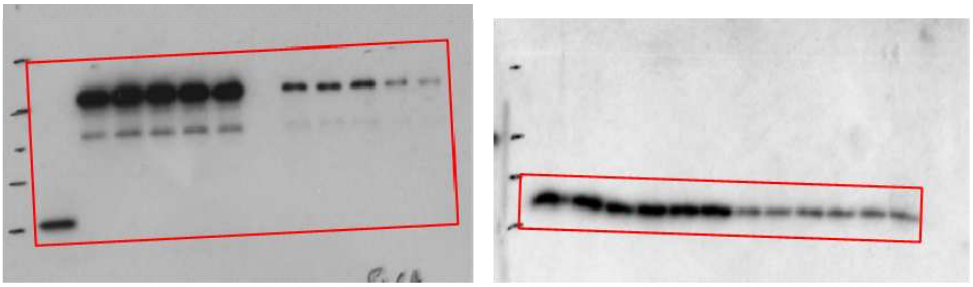

Figure 6b

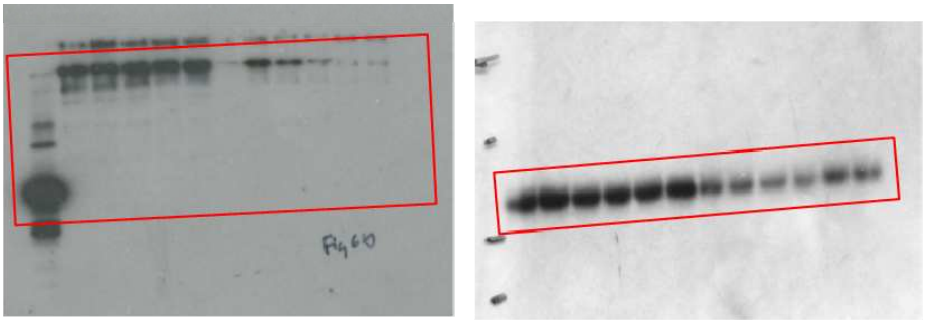

Supplementary Figure 1a

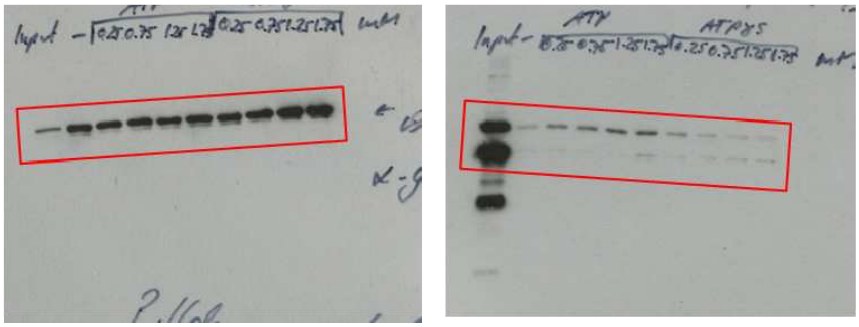

Supplementary Figure 1b

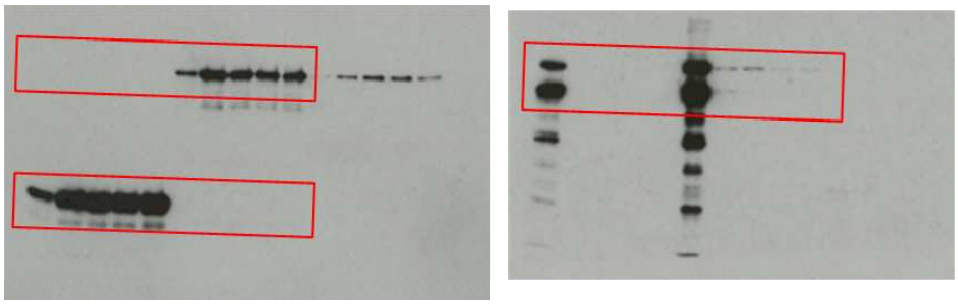

Supplementary Figure 14: Raw data presentation. Uncropped and unprocessed scans of all immunoblots. Labels indicate the corresponding figures, relevant bands are marked by the red box.

Supplementary Figure 3a

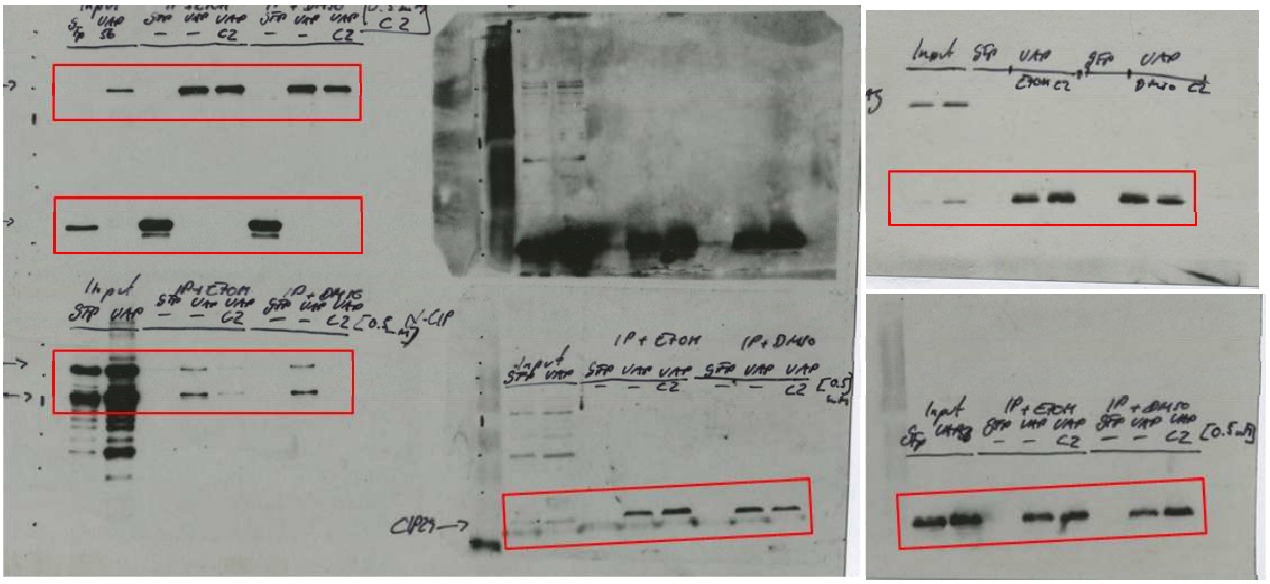

Supplementary Figure 3c

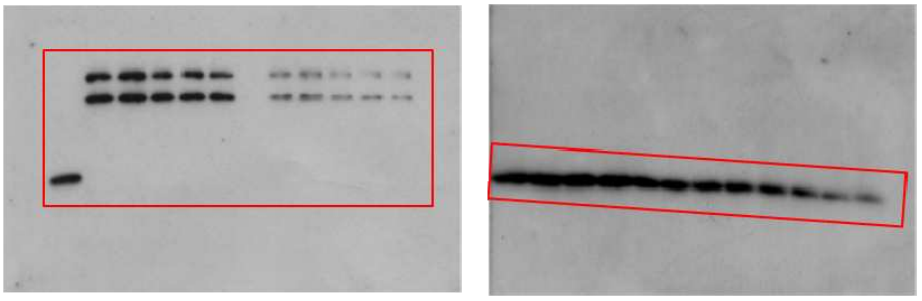

Supplementary Figure 4b

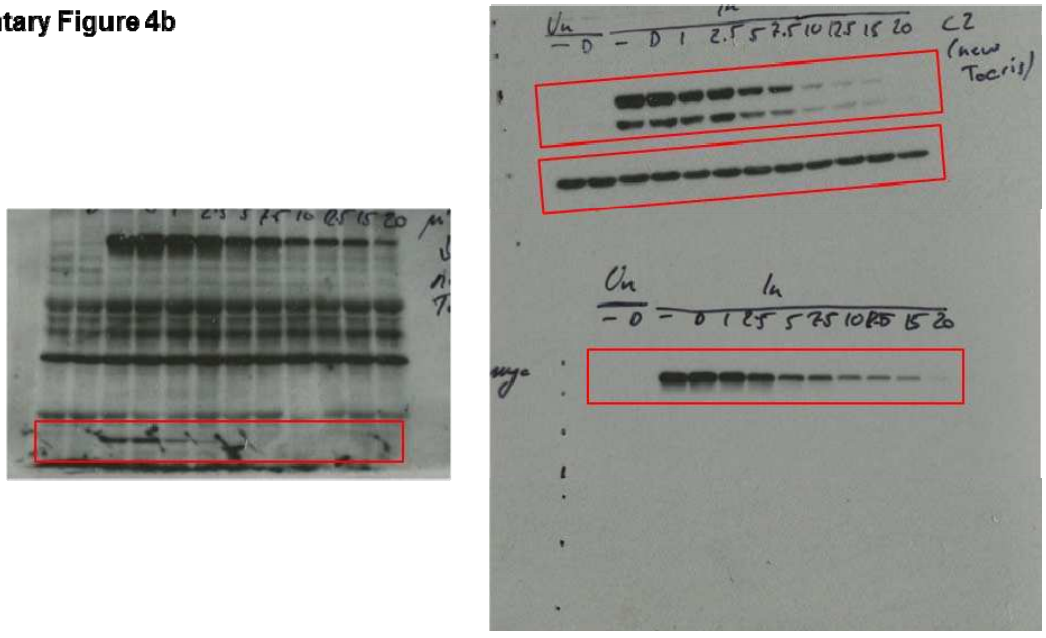

Supplementary Figure 14: Raw data presentation. Uncropped and unprocessed scans of all immunoblots. Labels indicate the corresponding figures, relevant bands are marked by the red box.

Supplementary Figure 4g

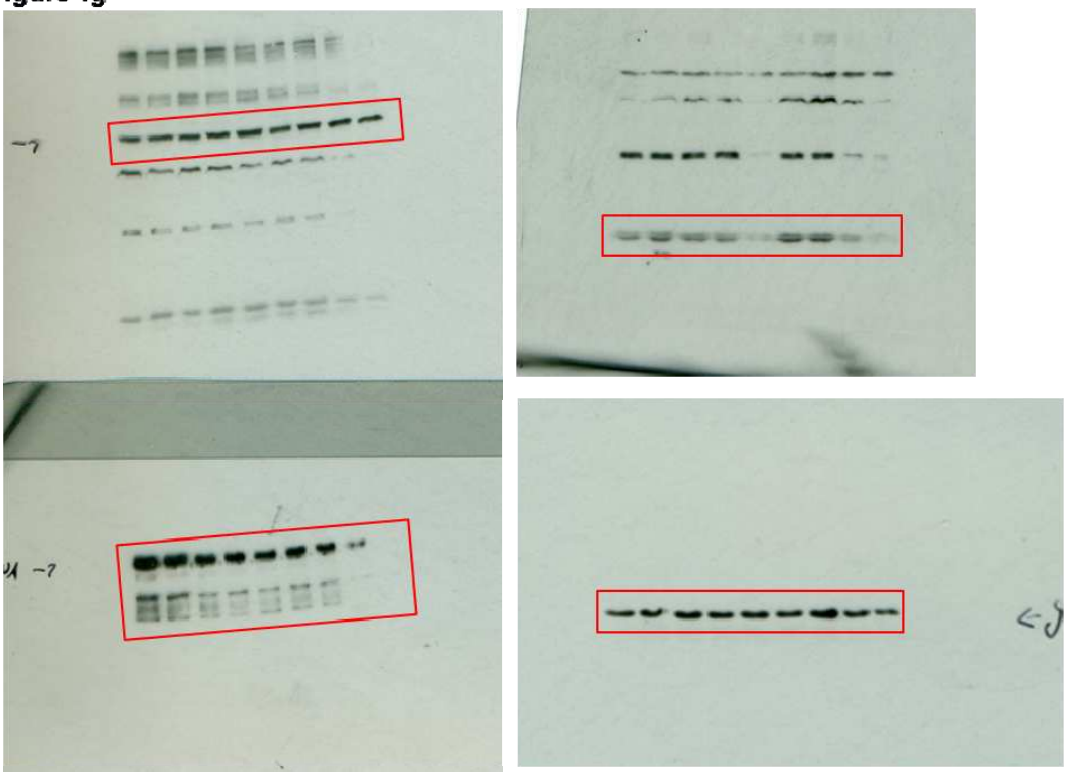

Supplementary Figure 5a

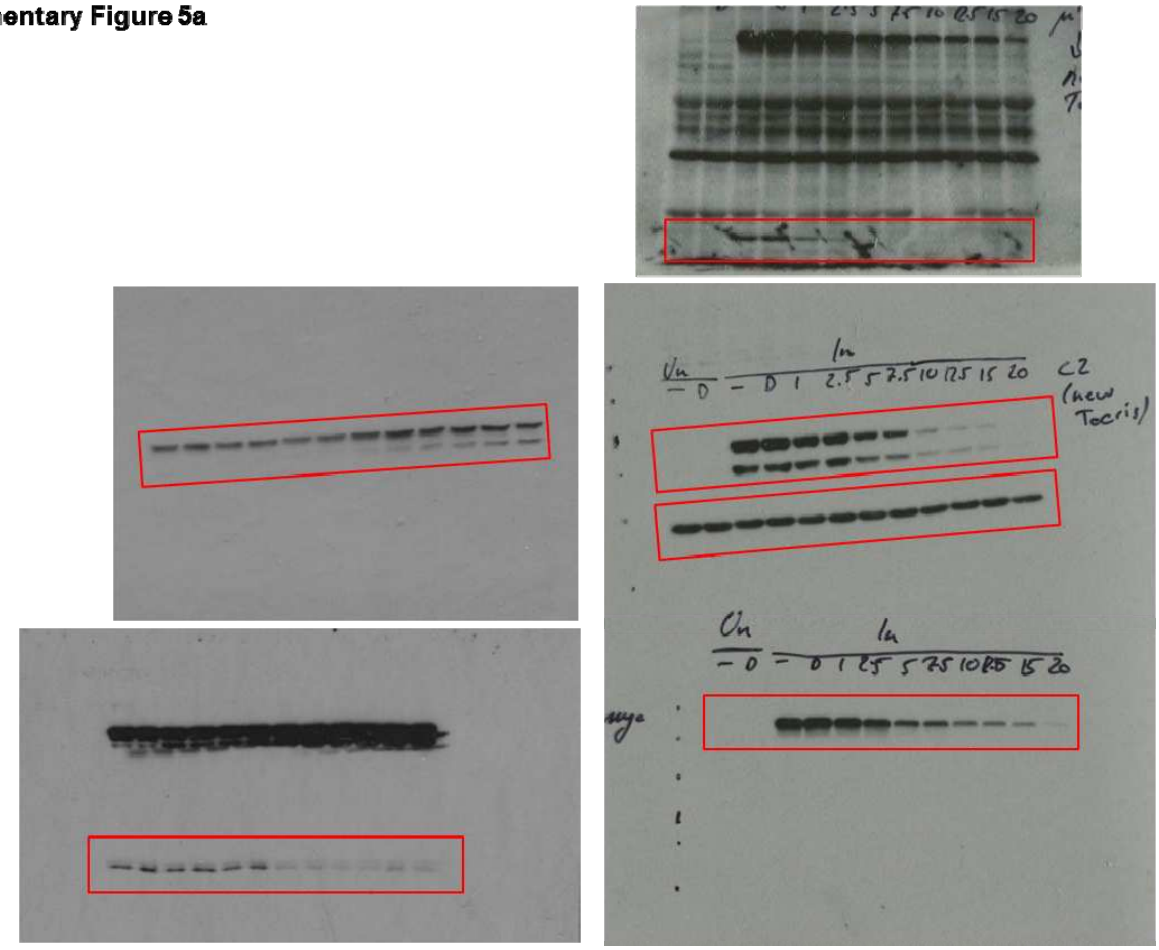

Supplementary Figure 14: Raw data presentation. Uncropped and unprocessed scans of all immunoblots. Labels indicate the corresponding figures, relevant bands are marked by the red box.

Supplementary Figure 6b

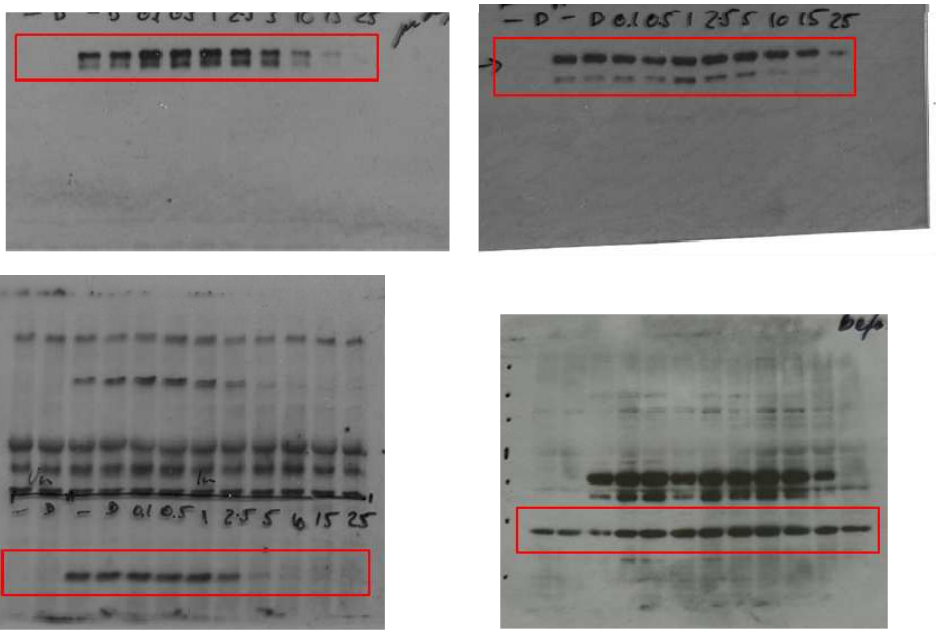

Supplementary Figure 6f

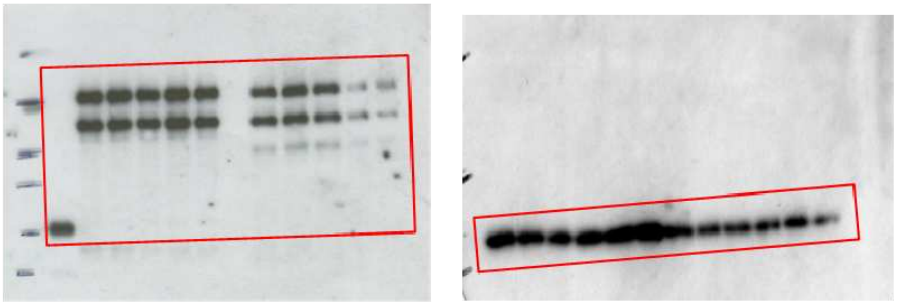

Supplementary Figure 7b

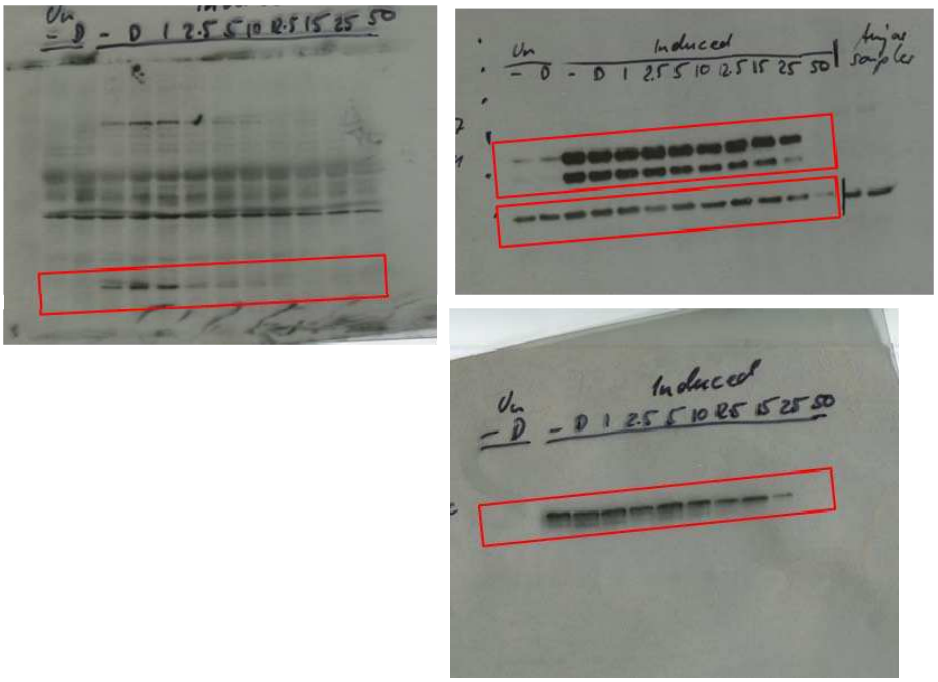

Supplementary Figure 14: Raw data presentation. Uncropped and unprocessed scans of all immunoblots. Labels indicate the corresponding figures, relevant bands are marked by the red box.

Supplementary Figure 7b

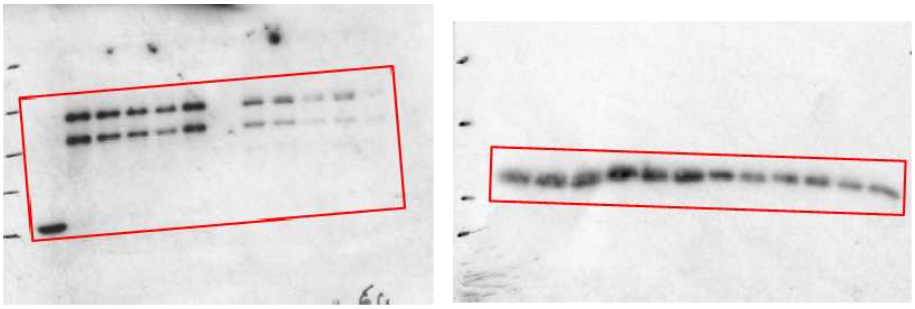

Supplementary Figure 8b

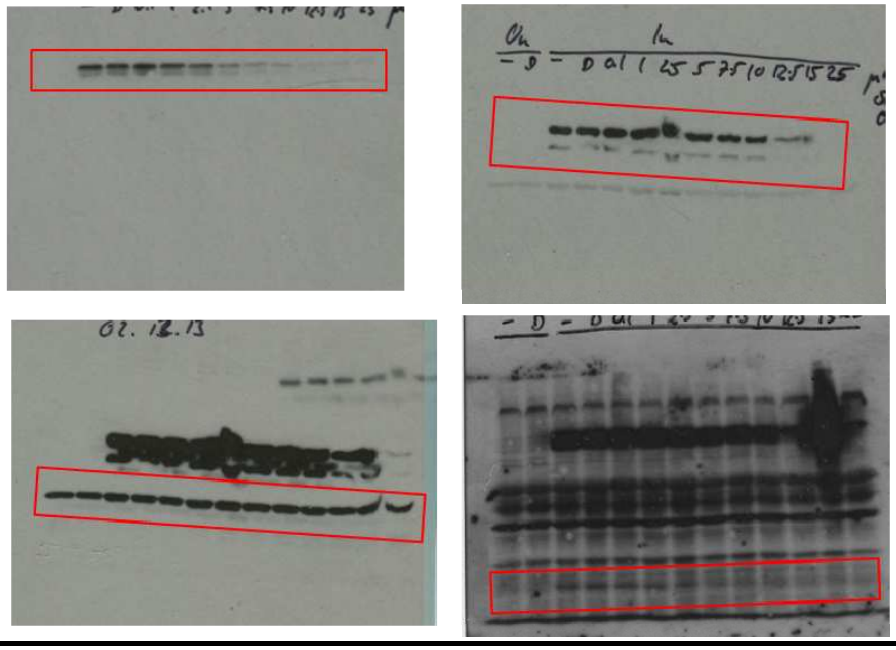

Supplementary Figure 8f

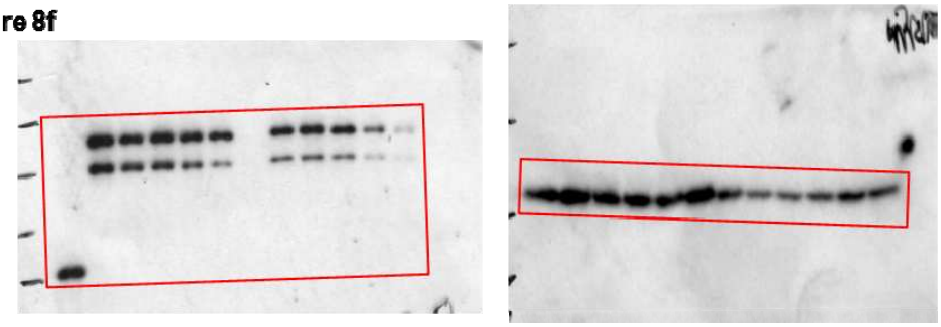

Supplementary Figure 14: Raw data presentation. Uncropped and unprocessed scans of all immunoblots. Labels indicate the corresponding figures, relevant bands are marked by the red box.

Supplementary Figure 9b

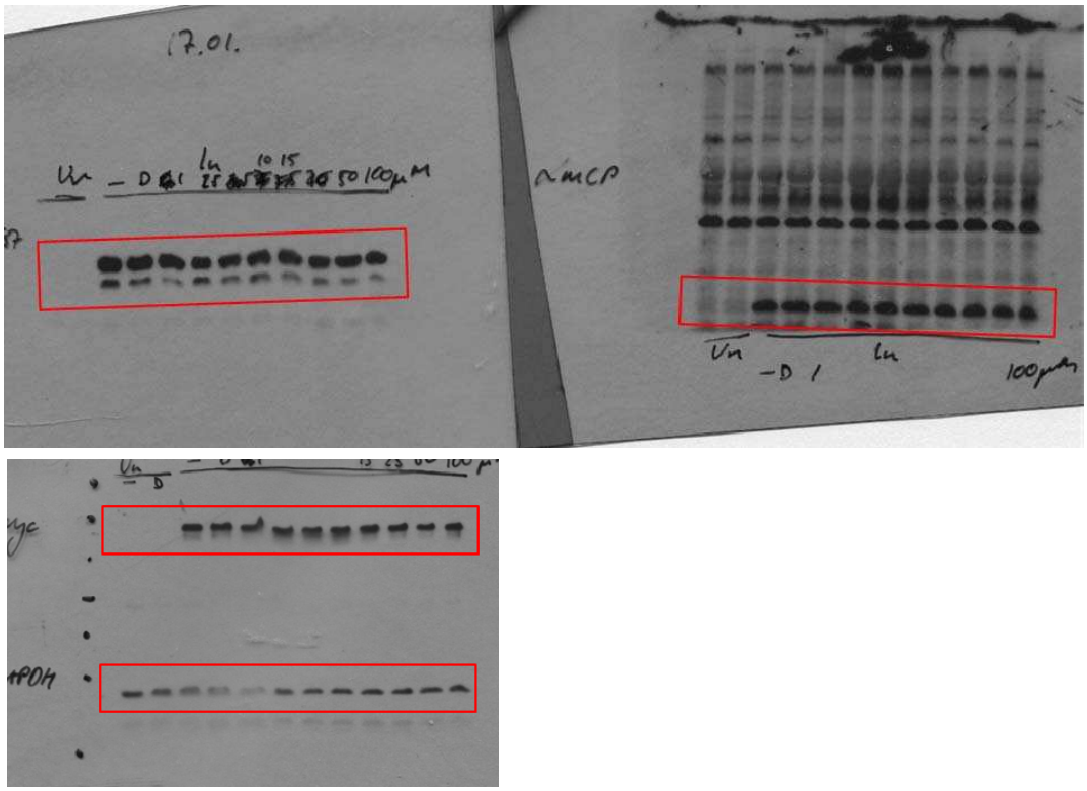

Supplementary Figure 10a

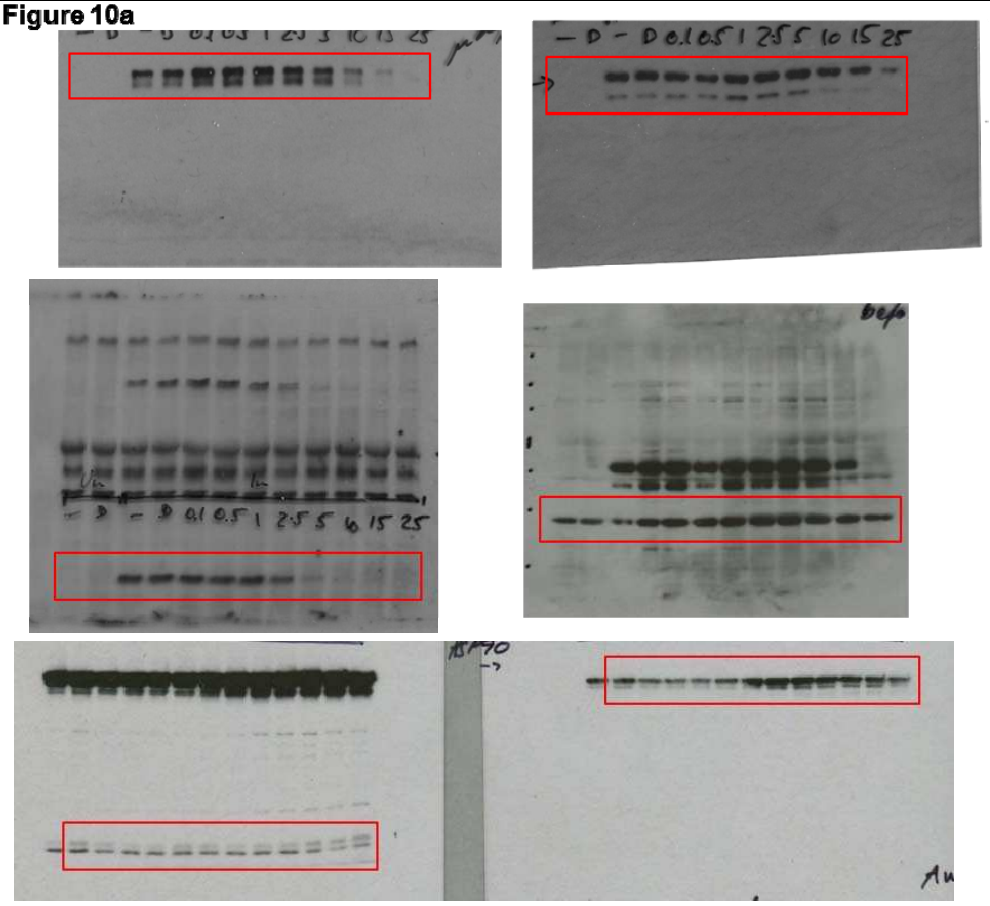

Supplementary Figure 14: Raw data presentation. Uncropped and unprocessed scans of all immunoblots. Labels indicate the corresponding figures, relevant bands are marked by the red box.

Supplementary Figure 11a

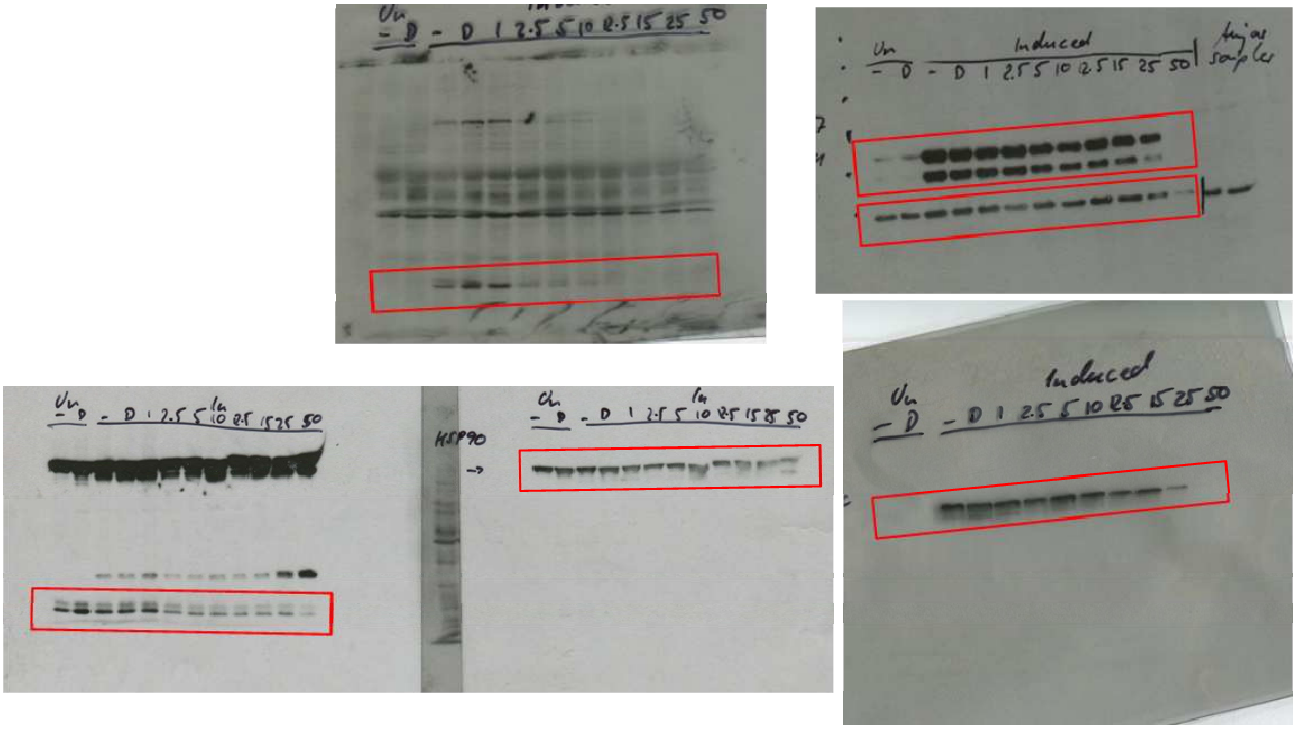

Supplementary Figure 12c

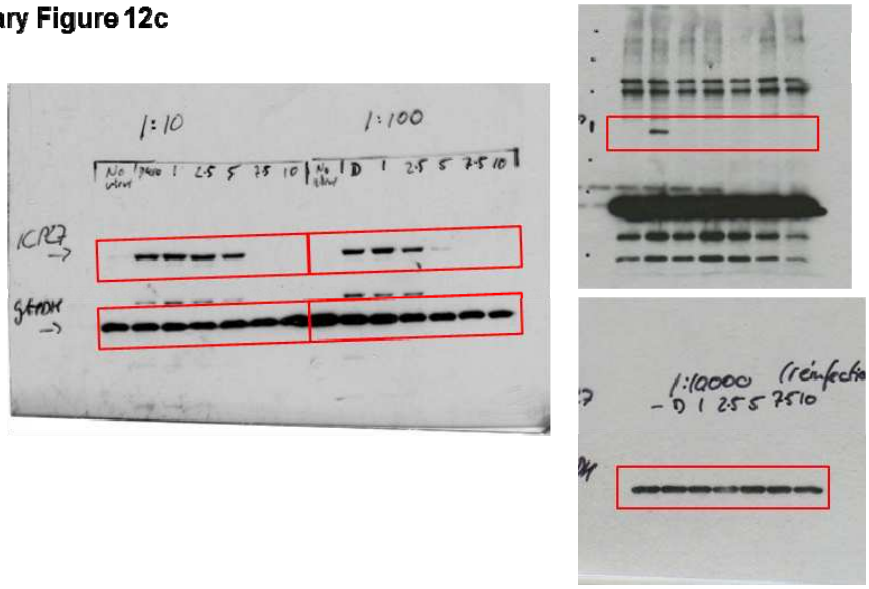

Supplementary Figure 13a

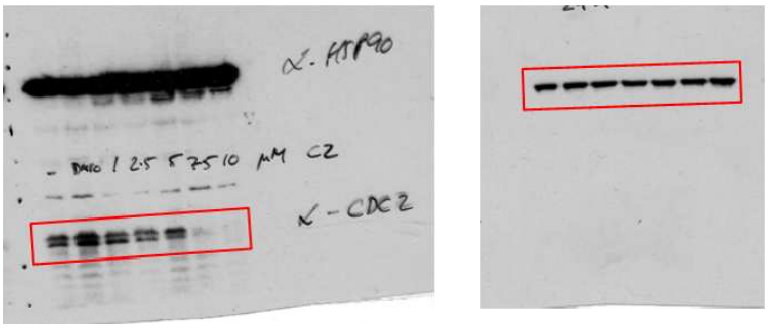

Supplementary Figure 14: Raw data presentation. Uncropped and unprocessed scans of all immunoblots. Labels indicate the corresponding figures, relevant bands are marked by the red box.